A consistent regional dataset of dissolved oxygen in the Western Mediterranean Sea (2004-2023): CTD-O$_2$WMED

Malek Belgacem[1], Katrin Schroeder[1], Marta Álvarez[2], Siv K. Lauvset[3], Jacopo Chiggiato[1], Mireno Borghini[4], Carolina Cantoni[5], Tiziana Ciuffardi[6], Stefania Sparnocchia[5]

[1] CNR-ISMAR, Arsenale Tesa 104, Castello 2737/F, 30122 Venice, Italy
[2] Instituto Español de Oceanografía, IEO-CSIC, A Coruña, Spain
[3] NORCE Norwegian Research Centre, Bjerknes Centre for Climate Research, Bergen, Norway
[4] CNR-ISMAR, Via Santa Teresa, Pozzuolo di Lerici, 19032 La Spezia, Italy
[5] CNR-ISMAR, Area Science Park, Basovizza, 34149 Trieste, Italy
[6] Department of Sustainability, St Teresa Marine Environment Research Centre, ENEA, Pozzuolo di Lerici, 19032 La Spezia, Italy

Correspondence to: Malek Belgacem (malek.belgacem@ve.ismar.cnr.it)

Abstract.

The Mediterranean Sea is experiencing rapid environmental changes, underscoring the urgent need for high-quality, long-term datasets to quantify trends and assess impacts on biogeochemical cycles. Over the past few years much work has been done to improve and ensure data quality in the Western Mediterranean Sea (WMED), but reliable dissolved oxygen (O$_2$) data remains scarce. This is a critical gap, as oxygen is a key indicator of marine ecosystem health and plays a central role in carbon and nutrient cycling. To address this gap, we compiled and rigorously quality-controlled a new regional-scale WMED dataset of O$_2$ data from sensors mounted on Conductivity Temperature and Depth (CTD) probes: CTD-O$_2$WMED. This product includes over 1000 previously unpublished high-resolution vertical profiles of CTD-O$_2$ measurements mostly collected within Italian cruises between 2004 and 2023. The quality control process involved sensor post-calibration against discrete Winkler measurements, primary screening, and a secondary check based on crossover analysis with reference datasets. Combined this ensures the consistency of the final corrected CTD-O$_2$WMED across both space and time. CTD-O$_2$WMED provides a robust observational foundation for assessing trends of dissolved oxygen variability, mainly associated with climate change, anomalies related to deoxygenation processes, and contributes to advancing our understanding of ventilation processes in the WMED. It also serves as a benchmark for calibrating biogeochemical Argo floats and for validating regional biogeochemical models.

Data coverage

Coverage: 44∘ N–35∘ S, 6∘ W–14∘ E
Location name: western Mediterranean Sea
Date/time start: October 2004
Date/time end: April 2023

1   Introduction

Dissolved oxygen (O_2) in the ocean is primarily produced through photosynthesis by phytoplankton in the surface layer, especially in regions of high primary productivity. The subsequent export and remineralization of organic matter from the surface lead to oxygen consumption at depth, potentially giving rise to oxygen minimum zones (OMZs) or oxygen minimum layers (OMLs), where biological respiration exceeds oxygen supply. While OMZs are characteristic of certain oceanic regions, the Mediterranean Sea is generally well-oxygenated and does not develop OMZs, but rather OMLs (Álvarez et al. 2022). Nonetheless, localized low-oxygen events may become more frequent and intense in response to ongoing climate change and human activities driving eutrophication events (Grégoire et al. 2023).

Ocean warming and increased stratification reduce oxygen solubility and inhibit vertical mixing, respectively, thereby limiting the downward transport of oxygen-rich surface waters. These processes contribute to the expansion and intensification of low-oxygen zones, with important consequences for biogeochemical cycling, ecosystem functioning, and carbon export (Keeling et a., 2009). In the deep ocean, enhanced remineralization and reduced ventilation can further exacerbate oxygen loss. Under low-oxygen conditions, denitrification may also occur, altering the nitrogen-to-phosphorus (N:P) ratio and influencing both nutrient cycling and primary productivity.

Increased CO_2 concentrations and stratification can also reshape biological communities, potentially lowering ecosystem resilience. These biogeochemical shifts affect the distribution of oxygen and other biogeochemical variables, particularly in semi-enclosed basins like the Mediterranean Sea. In recent decades, the region has undergone significant environmental changes, including recurrent marine heatwaves (Marullo et al., 2023; Martinez et al., 2023; Pastor and Khodayar et al., 2023), which influence oxygen distribution (Reale et al., 2022; Alvarez et al., 2023). The Mediterranean's semi-enclosed configuration, complex thermohaline circulation, and pronounced regional differences make it especially sensitivity to climate variability (Powley et al., 2016; Testor et al., 2017; Margirier et al., 2020).

Two major events have notably impacted the thermohaline structure of the Mediterranean Sea. In the Eastern Mediterranean (EMED), the Eastern Mediterranean Transient (EMT) of the mid-1990s shifted deep-water formation source from colder, less saline Adriatic Deep Water to warmer, saltier Aegean/Cretan Water. This new deep-water mass ventilated the Levantine basin and the Ionian Sea around 1999 and reached the Sicily Channel by 2001 (Schroeder et al., 2006). When the Aegean contribution weakened, the Adriatic source regained dominance between 2000 and 2010. However, in subsequent years, it failed to reach the deepest Ionian layers, ventilating instead the 2000-3000 m depth range. In the Western Mediterranean Sea (WMED), deep convection in the Gulf of Lion has traditionally ensured ventilation of the Western Mediterranean Deep Water (WMDW). A peak in deep water renewal occurred during the Western Mediterranean Transition (WMT) in year 2005 (Schroeder et al., 2016). Since then, a decline in both frequency and intensity of deep convection has been observed (Fourrier et al., 2020; Li and Tanhua, 2020), leading to reduced deep layer ventilation and an intensification of the oxygen minimum at intermediate depths, with implications for the uptake of atmospheric oxygen (Ulses et al., 2021). Long-term observational programs such as the MEDAR/MEDATLAS (Fichaut et al., 2003), Med-SHIP (Schroeder et al., 2015), RADMED (López-Jurado et al., 2015), and the MOOSE network (Coppola et al., 2018) have provided crucial insights into these changes. Recently, machine learning techniques have been employed to

78 reconstruct oxygen fields at higher spatial and temporal resolution using satellite and auxiliary data sources (Liu
79 et al., 2025). Nevertheless, substantial uncertainties in the quantification and long-term impacts of O2 changes on
80 Mediterranean Sea marine ecosystems still remain (Coppola et al., 2018; Alvarez et al. 2014).

81 To improve our understanding of regional dissolved oxygen dynamics and the impact of climate changes on
82 biogeochemical trends, this study presents a quality-controlled compilation of CTD oxygen profiles collected by
83 the Italian National Research Council (CNR) between 2004 and 2023 in the WMED. The dataset provides reliable
84 CTD-based oxygen measurements that support assessments of water mass ventilation and long-term variability.
85 This paper documents the dataset and outlines the quality control procedures, including calibration assessment
86 against discrete Winkler measurements, first quality control flagging and secondary quality corrections, to ensure
87 the consistency of the CTD oxygen data product released, CTD-O$_2$WMED.

2 Dissolved oxygen data collection

2.1 The CNR data collection

90 The CTD-Oxygen in the WMED (CTD-O$_2$WMED) dataset comprises 1382 dissolved oxygen profiles collected
91 with CTD probes across 25 CNR research cruises (Table 1). Figure 1 shows the spatial distribution of these
92 profiles, illustrating broad coverage throughout the northern WMED and along key hydrographic transects. The
93 majority of measurements are concentrated in the eastern portion of the WMED, including the Ligurian and
94 Tyrrhenian Seas, and the Tunisia-Sicily-Sardinia region.
95 Spanning the period from 2004 to 2023, the dataset provides robust temporal coverage, particularly from 2004 to
96 2015 (see Figure 2a). Notably, the years 2005, 2006, 2010, and 2012 comprise the highest number of CTD stations,
97 coinciding with monthly surveys (Figure 2). While the temporal distribution remains consistent between 2004 and
98 2015 (except for 2014), the number of sampled stations decreases significantly after 2016.

99
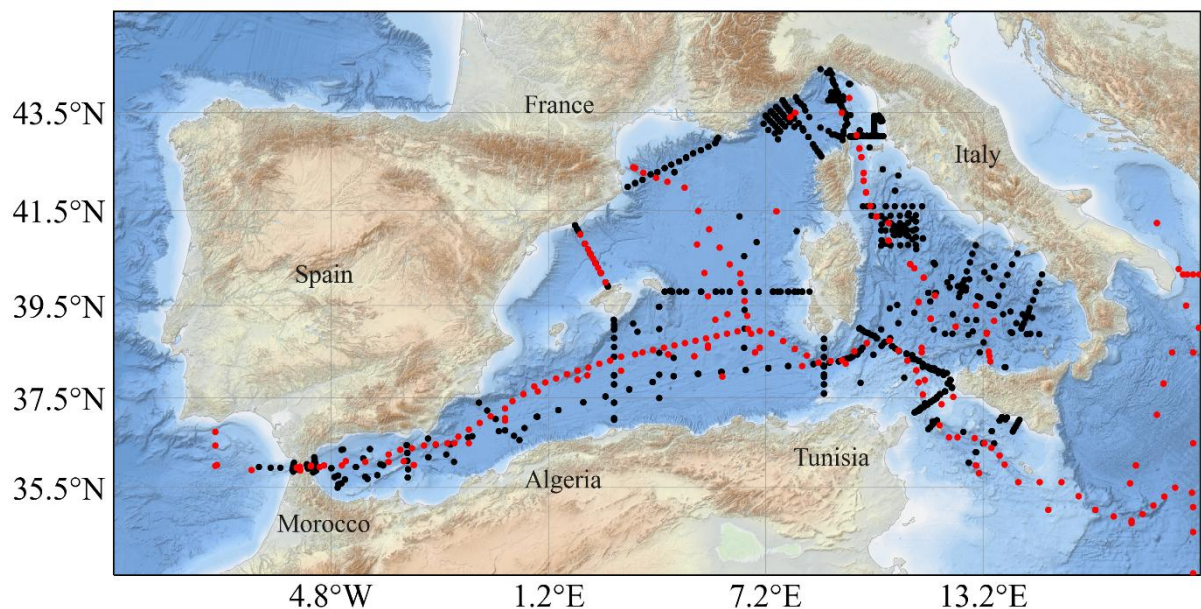
100 **Figure 1.** Spatial distribution of cruise stations with CTD oxygen data (black dots) in the CTD-O$_2$WMED dataset.
101 The red markers indicate stations (discrete Winkler measurements) from the reference dataset.

102

(a)

(b)
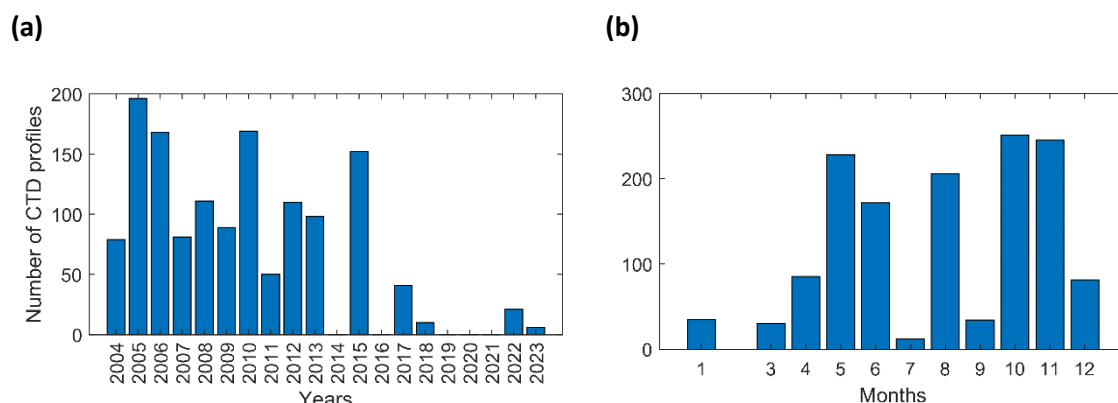
Figure 2. Temporal information about CTD-O$_2$WMED profiles: (a) annual and (b) monthly distributions.

2.2 Assessment of CTD-O$_2$ post-calibration

CTD-O2, which stands for sensor based dissolved oxygen, was measured using Sea-Bird SBE43 sensors mounted on the CTD rosette frame. For each cruise, all variable were checked and converted to standard units to ensure uniformity. Dissolved oxygen was the converted from milliliters per liter (ml L^{-1}) to micromoles per kilogram (µmol/kg) using potential density and the conversion factor 44.66 µmol O$_2$ L^{-1}, ensuring consistency across datasets. In addition, discrete samples collected at various depths from Niskin bottles were analyzed via Winkler titration onboard. This dataset focuses exclusively on CTD sensor data, so the discrete data are not included in the final product.

The Gibbs Sea Water (GSW) toolbox (https://www.teos-10.org/pubs/gsw/html/gsw_contents.html) was used to compute conservative temperature (CT), absolute salinity (SA), and potential density to provide an accurate representation of seawater properties during the 1st quality check process.

In the second step the CTD-O$_2$ data from cruises listed in Table 1 were post-calibrated using Winkler discrete data, following standard protocols (Grasshoff et al. 1983; Langdon, 2010) and accounting for sensor drift and hysteresis in line with the procedures by Janzen et al. (2007) and Uchida et al. (2010). We followed the Sea-Bird Electronics Application Note 64-2 (*SBE 43 DO Sensor calibration and data correction*, www.seabird.com). Residuals between the Winkler (O$_2$ bottle) and sensor CTD (O$_2$ sensor) measurements, matched based on pressure, were evaluated after post-calibration, following Uchida et al. (2010) (Figure 3). When more than one SBE43 sensor was deployed during a cruise, the sensor with the lowest residuals relative to Winkler samples was used in the further assessment.

Figure 3a shows the residuals (O$_2$ bottle – O$_2$ sensor) plotted against pressure, with cruises color-coded by start date. Differences of up to ±10 µmol/kg are observed especially in the upper 800 dbars. Figure 3b summarizes residual distributions for each cruise using whisker plots, where it is easy to identify cruises with high variability (standard deviation of the mean residual > 7 µmol/kg): 48UR20041006, 48UR20050412, 48UR20080905, and 48QL20171023. For cruise 48UR20080905, only five Winkler samples were available, which limited the post-calibration quality. In cruise 48UR20050412, which comprised two legs, discrete samples from only one leg were used for the entire cruise calibration, further affecting quality of the CTD-O$_2$ data. Figure 3c summarizes the cruise-level agreement using mean residuals and the percentage of residual values within ±2 µmol/kg. Following Uchida et al. (2010), residuals within this threshold are considered acceptable. Cruises were categorized as follows: green:

133 ≥40% of residuals within ±2 µmol/kg (good agreement); blue: 19–39% of residuals within ±2 µmol/kg (moderate

134 or uncertain agreement); grey: <19% of residuals within ±2 µmol/kg (poor agreement and probably systematic

135 bias in CTD-O$_2$ data). Eight cruises showed good agreement, eleven were moderate, and the remainder exhibited

136 systematic positive or negative biases, as pointed by the mean value of the residuals (Figure 3c). These deviations

137 may reflect sensor drift, post-calibration issues, or bottle-handling errors.

(a)

(b)

(c)
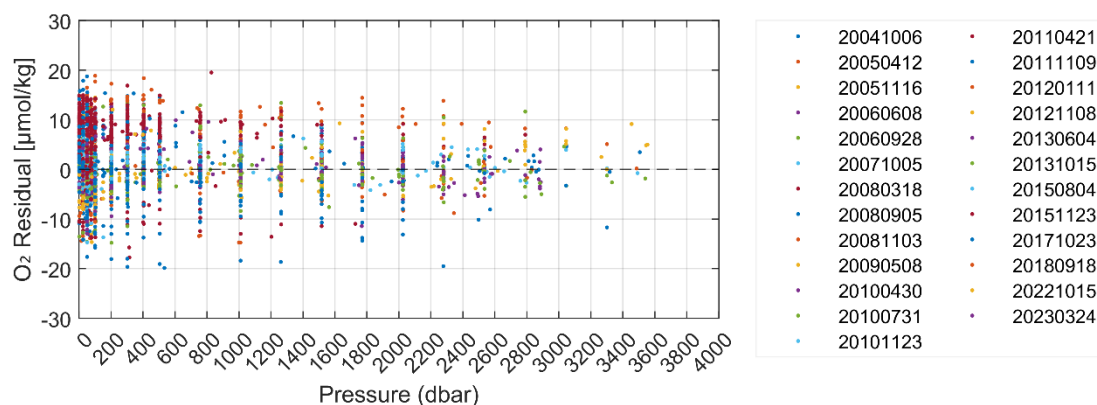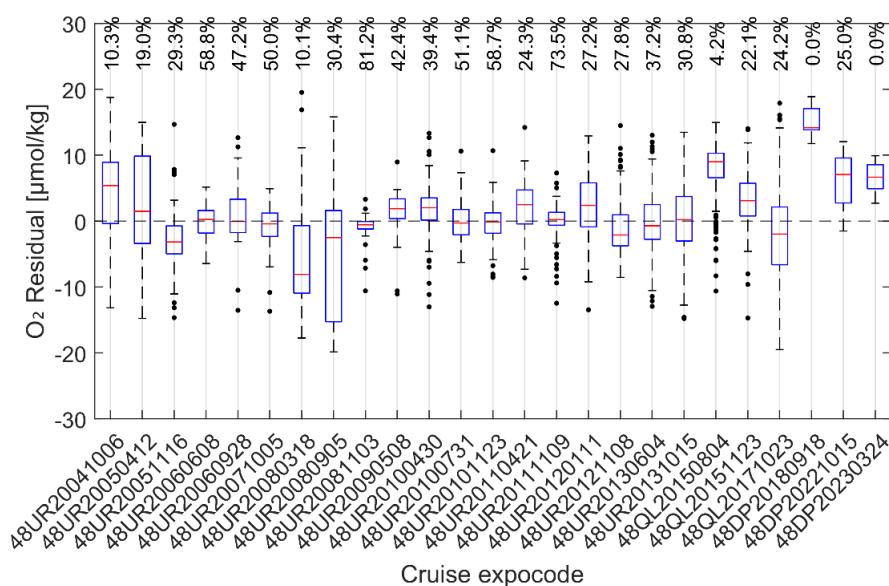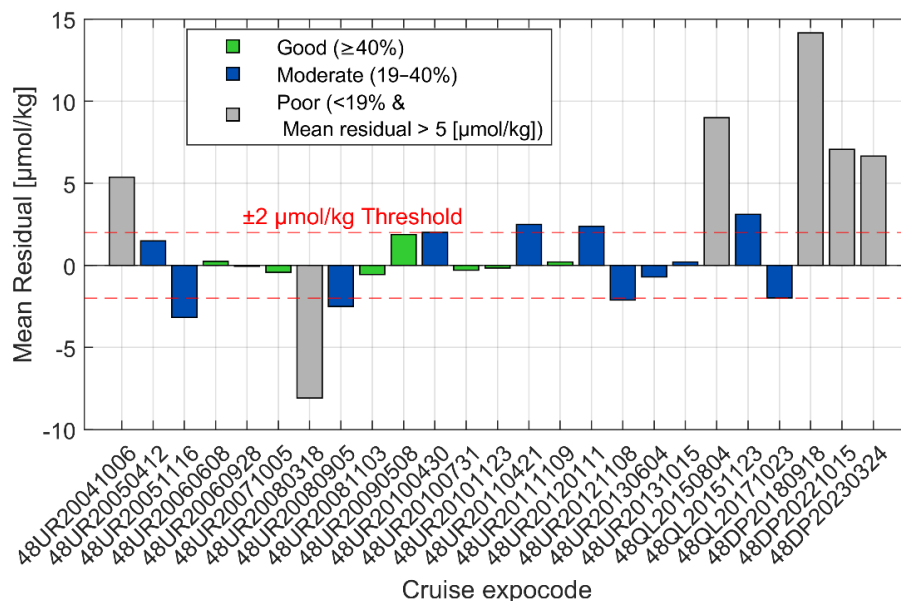
138 **Figure 3.** Residual values by cruise, showing the difference between CTD oxygen data (O_2 sensor) and Winkler
139 oxygen data (O_2 bottle): (a) against pressure with each cruise identified with the starting date; (b) whisker plot
140 with additional information about the % of data with residual values within ±2 µmol/kg for each cruise identified
141 with the expocode, and, (c) general assessment of each cruise, identified with the expocode, depending on the
142 value of the mean residual and the % of residual values withing ±2 µmol/kg.

143

144 **Table 1.** Cruises contained in the CTD-O_2WMED data product; for each cruise, the alias, expocode, research
145 vessel and date information are provided, along with the number of stations with CTD-O_2 profiles (Nb). Refer to
146 Table S1, Belgacem et al. (2020) and Ribotti et al. (2022) for additional cruise metadata.

Cruise ID	Cruise Alias	Expocode	Research Vessel (RV)	Date Start/End	Nb CTD profile
2	MEDGOOS9	48UR20041006	Urania	6 - 25 OCT 2004	82
3	MEDOCC05/ MFSTEP2	48UR20050412	Urania	24 APR - 16 MAY 2005	160
5	MEDGOOS11	48UR20051116	Urania	16 NOV - 3 DEC 2005	36
6	MEDOCC06	48UR20060608	Urania	8 JUN - 3 JUL 2006	127
8	MEDGOOS13/MEDBIO06	48UR20060928	Urania	28 SEP - 8 NOV 2006	41
9	MEDOCC07	48UR20071005	Urania	5 - 29 OCT 2007	81
10	SESAMEIt4 KM3	48UR20080318	Urania	18 MAR - 7 APR 2008	27
11	SESAMEIT5	48UR20080905	Urania	5 - 16 SEP 2008	24
12	MEDCO08	48UR20081103	Urania	3 - 24 NOV 2008	60
13	TYRRMOUNTS	48UR20090508	Urania	8 MAY - 3 JUN 2009	86
14	BIOFUN010	48UR20100430	Urania	30 APR - 17 MAY 2010	29
15	VENUS1	48UR20100731	Urania	31 JUL - 25 AUG 2010	116
16	BONSIC2010	48UR20101123	Urania	23 NOV - 9 DEC 2010	24
17	EUROFLEET11	48UR20110421	Urania	21 APR - 8 MAY 2011	31
18	BONIFACIO2011	48UR20111109	Urania	9 - 23 NOV 2011	18
20	ICHNUSSA12	48UR20120111	Urania	11 - 27 JAN 2012	35
21	EUROFLEET2012	48UR20121108	Urania	8 - 26 NOV 2012	75
211	VENUS 2	48UR20130604	Urania	4 - 25 JUN 2013	59
22	ICHNUSSA13	48UR20131015	Urania	15 - 29 OCT 2013	40
222	ICHNUSSA15	48QL20151123	Minerva Uno	23 NOV - 14 DEC 2015	62
23	OCEANCERTAIN15	48QL20150804	Minerva Uno	4 - 18 AUG 2015	90
24	ICHNUSSA17/INFRAOCE17	48QL20171023	Minerva Uno	23 OCT- 28 NOV 2017	41
25	ICHNUSSA/JERICO18	48DP20180918	DallaPorta	18-25 SEP 2018	10
27	JERICO-II-2022	48DP20221015	DallaPorta	15- 25 OCT 2022	21
28	JERICO-III-EurogoShip-2023	48DP20230324	DallaPorta	24 MAR - 09 APR 2023	6

147

3 Primary and secondary quality control methods

3.1 Reference cruises with Winkler dissolved oxygen data in the WMED

An external reference data set for dissolved oxygen discrete measurements was used to compare the CNR CTD-O_2WMED data. Discrete Winkler measurements on those reference cruises (Table 2, Figure 4) were performed following the GO-SHIP (Global Ocean Ship-Based Hydrographic Investigations Program) protocol ensuring robust O2 data quality to better than 1 µmol/kg (Langdon, 2010). Among these reference, cruises 06MT20011018 and 06MT20110405 are significant surveys, contributing to the GLODAPv2 data product (Olsen et al., 2016; 2020). They underwent full quality control with no bias correction applied to the original data. Similarly cruises 48UR20070528, 29AH20140426, and 06M220180302, which are being assembled into the consistent carbon and ancillary dataset CARIMED (CARbon, tracer, and ancillary data In the MEDsea, Alvarez et al., 2019), have been rigorously quality controlled (Álvarez et al., in preparation). Cruises 29AJ20160818 and 11BG20220517 conducted in 2016 and 2022 (Tanhua, 2019a, 2019b; Jullion, 2016; Schroeder, 2022; Schroeder et al., 2024) followed GO-SHIP protocols under the Med-SHIP (Mediterranean Sea repeat hydrography) framework, which emphasizes the collection of high-quality hydrographic and biogeochemical data for long-term climate studies (Schroeder et al., 2015, 2024). These seven reference cruises were selected based on data quality and geographic overlap with the CTD-O_2WMED dataset. Figures 1 and 5 shows the regional distribution of the reference data, which aligns well with the CTD-O_2WMED cruise tracks, particularly in the Tyrrhenian Sea and Algerian basin which are the two most frequently sampled subregions.

Table 2. Overview of reference cruise datasets with high quality Winkler oxygen measurements, including expocode. The dataset covers the period from 2001 to 2022.

Cruise Alias	EXPOCODE	Date starts and end	Stations	Source	Chief scientist(s)
M51/2	06MT20011018	*18 Oct–11 Nov 2001*	6	GLODAPv2	Wolfgang Roether
TRANSMED_LEGII	48UR20070528	*28 May–12 Jun 2007*	4	CARIMED	Maurizo Azzaro
M84/3	06MT20110405	*5–28 Apr 2011*	20	GLODAPv2	Toste Tanhua
HOTMIX	29AH20140426	*26 Apr–31 May 2014*	18	CARIMED	Javier Aristegui
TAlPro-2016	29AJ20160818	*18–28 Aug 2016*	42	Med-SHIP	Loïc Jullion
MSM72	06M220180302	*2 Mar–3 Apr 2018*	130	GO-SHIP	Dagmar Hainbucher
TAlPro-2022	11BG20220517	17-26 May 2022	24	Med-SHIP	Katrin Schroeder
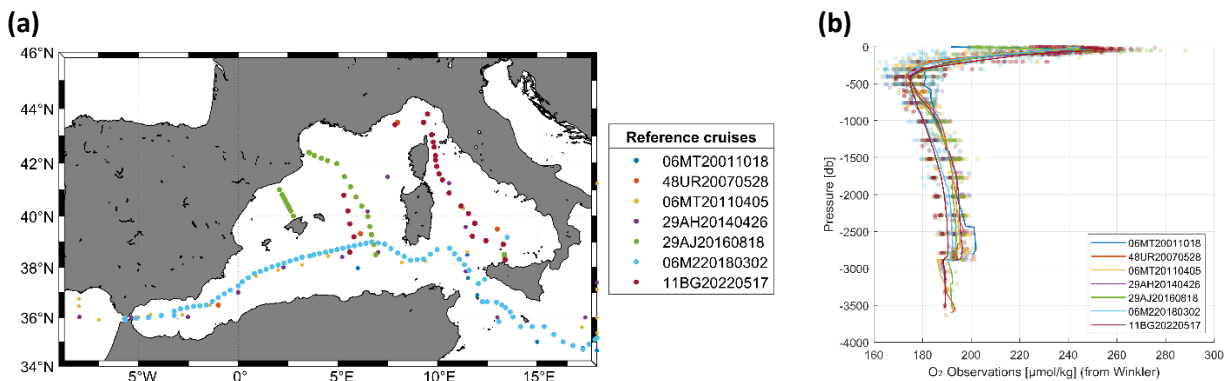
(c)
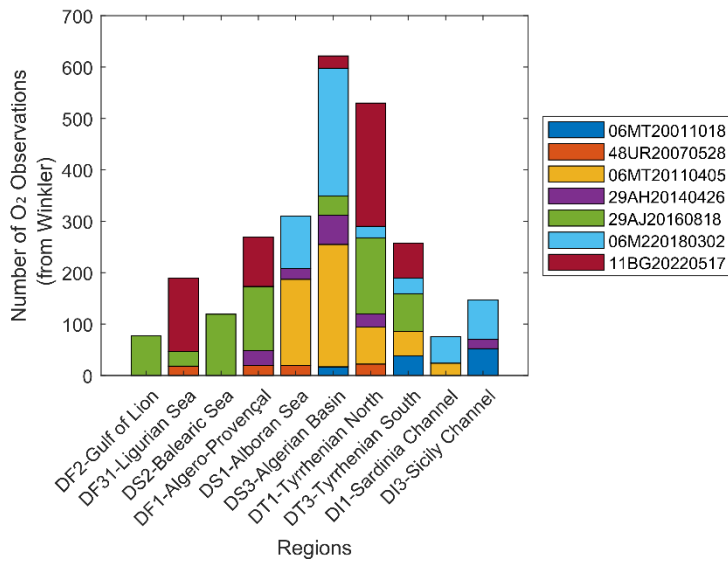
Figure 4. Reference cruises: (a) Map showing the location of reference stations; (b) vertical distribution of dissolved oxygen data from Winkler measurements, including the mean profile across all reference cruises; and (c) number of reference oxygen observations (Winkler measurements) per region.

3.2 Primary quality control of CTD-O$_2$ data

Following unit conversion and post-calibration with Winkler measurements (section 2.2), each cruise underwent an outlier screening process. Data quality flags were assigned following the WOCE standards: flag 2 for acceptable values, flag 3 for questionable values, flag 4 for bad values, and flag 9 for missing or not measured data. Flagging was tailored to the expected accuracy and precision of CTD-O$_2$ data for each individual cruise, which depends on the available measurements for Winkler oxygen and the stability of the CTD-O$_2$ sensor. Note that metadata information was scarce for some cruises. Property-property plots were analyzed for each region, and CTD-O$_2$ values identified as outliers in multiple plots were flagged as questionable. Approximately 0.2% of the CTD-O$_2$ data were flagged as outliers (flag 3). The 1st QC is inherently subjective, relying on the expertise of the analyst reviewing the data.

3.3 Overview and first assessment on CTD-O$_2$ WMED data

To illustrate the regional oxygen distribution, Figure 5a presents the vertical CTD-O$_2$WMED profiles by pressure across ten WMED subregions defined in Figure 5b according to Manca et al. (2004). Gray lines show the full dataset, while blue lines indicate the range of oxygen concentrations in each subregion, revealing clear spatial and vertical patterns. The vertical distribution of dissolved oxygen in the WMED reflects a balance between air-sea gas exchange, biological activity, and regional circulation. Surface concentrations remain near atmospheric saturation due to gas exchange and photosynthesis activity. As organic matter sinks and is remineralized, oxygen is consumed at depth, generating vertical gradients. Unlike other ocean basins where pronounced OMZs develop, the WMED remain relatively well-oxygenated, thanks to episodic deep convection in the Gulf of Lion. This process ventilates the WMDW, which then spreads across subregions including the Algerian basin and Ligurian Sea, known to be among the best-ventilated areas (Schneider et al., 2014).

In the WMED, a recurrent feature is the intermediate OML, typically found between 300 and 600 db. This layer coincides with the core of the Eastern Intermediate Water (EIW), which is warmer, saltier, and consistently lower in oxygen than surrounding waters (Tanhua et al., 2013; Coppola et al., 2018; Mavropoulou et al., 2020). The OML's depth, thickness, and intensity vary by region and year, depending on remineralization rates, mixing, and circulation (Coppola et al., 2018). In the Tyrrhenian subregion (DT3, DT1), the oxygen increases again below the OML, suggesting the influence of deeper, more oxygenated waters. In contrast, the lowest oxygen levels in the WMED are found in the Sicily Channel (DI3) and Tyrrhenian Sea (DT3, DT1), where the EIW is prominent and deep ventilation is absent. The Alboran (DS1) and Balearic (DS2) Seas, by contrast, show relatively well-oxygenated profiles throughout the water column. This reflects both the presence of WMDW and enhanced vertical transport due to mesoscale and submesoscale processes that facilitate the downward movement of oxygen-rich surface waters (Middleton et al., 2025).

(a)
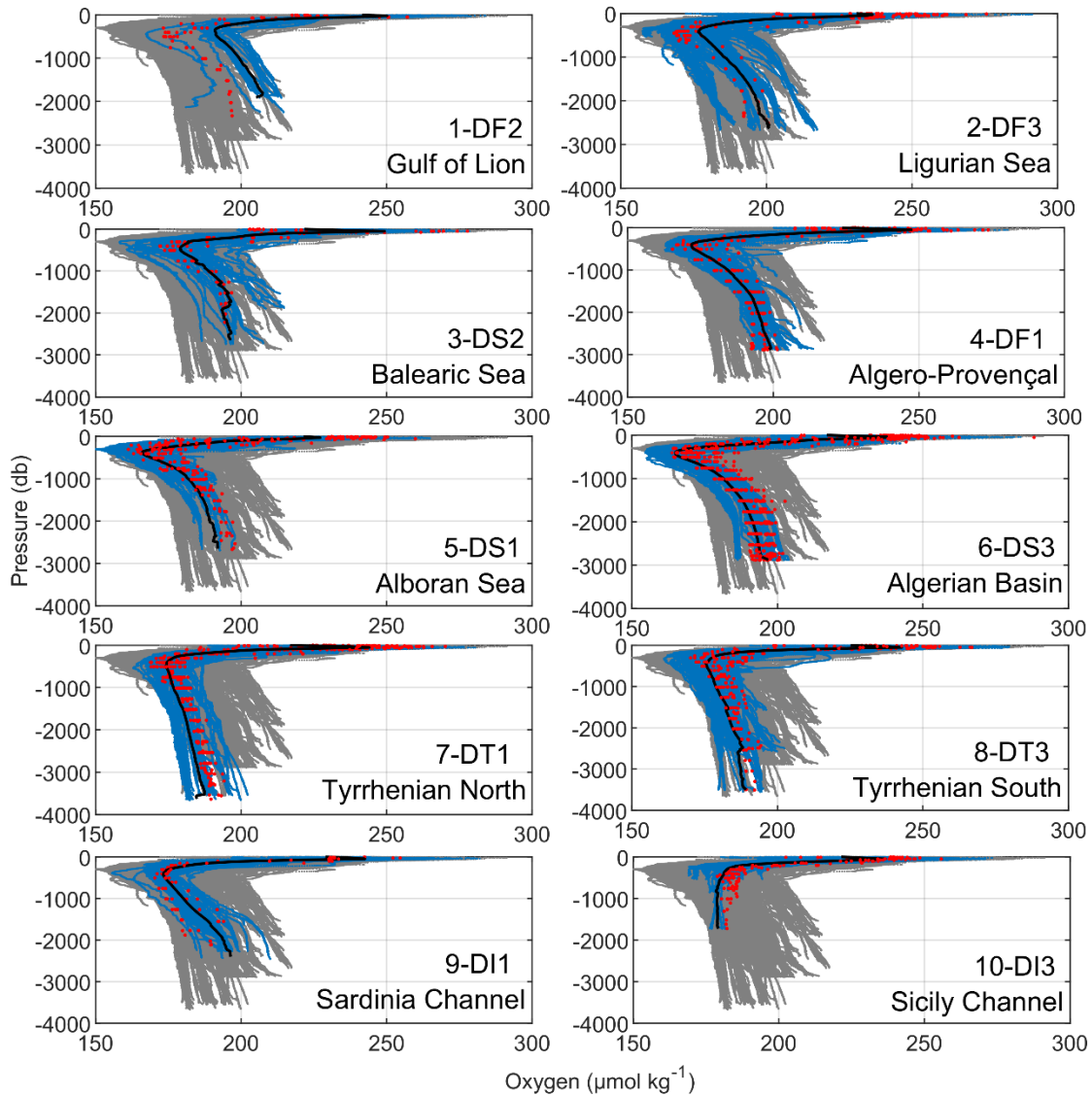
(b)
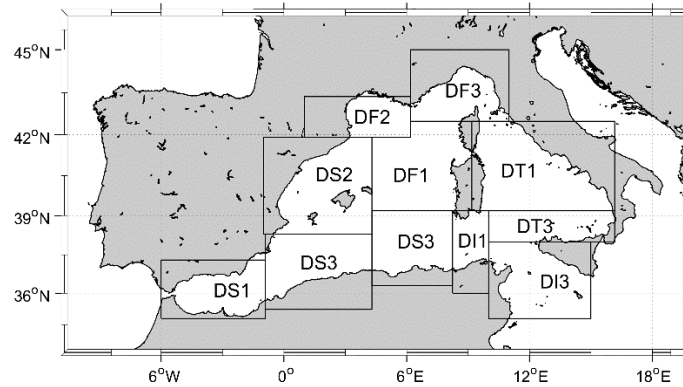
Figure 5. (a) Vertical distribution of CTD-O$_2$ (µmol/kg) versus pressure across the WMED. Grey profiles represent individual stations from the full dataset after initial quality control (1st QC). Blue shading shows the oxygen concentration envelope within each subregion (see Table S2), while black lines indicate the subregional mean profiles averaged over the entire period. Red dots represent selected reference profiles used for comparative analysis. (b) Map showing the geographic boundaries of the MEDAR/MEDATLAS subregions used in this study (see Table S2), adapted from Manca et al. (2004).

In order to assess the internal consistency and precision of the CTD-O$_2$WMED data across CNR cruises, we computed for each cruise the median and median absolute deviation (MAD) of deep oxygen values flagged as good (depth > 800 dbar, see Figure 6 and Table S3, in the Supplementary Material). This approach minimizes the influence of atmospheric forcing, mesoscale variability and residual outliers. Figure 6a illustrates the spatial variability in deep-water oxygen concentrations across the WMED. A pronounced east-west gradient is evident, with lower oxygen levels (blue tones) in eastern subregions such as the Tyrrhenian Sea, Sardinia Channel, and Sicily Channel, and higher oxygen levels (green to yellow) in western regions, where deep convection processes in the Gulf of Lion enhance ventilation. The MAD was used as a proxy for precision, and overall MAD values ranged from 0.1 to 7.5 µmol/kg. In well-sampled subregions (≥5 cruises) high MAD values or anomalous medians were used to identify potentially biased CTD-O$_2$ cruises.

Below we summarize the findings by subregion:

- Ligurian Sea (DF3): of the five cruises, cruise #3 (48UR20050412) and #21 (48UR20121108) had the highest MAD. Cruise #2 (48UR20041006) had a median consistent with the others, but cruise #3 was ~10 µmol/kg lower, and cruise #6 was 16 µmol/kg higher, despite a low MAD, suggesting possible bias or calibration errors.
- Balearic Sea (DS2): among the six cruises, all but cruises #3 (48UR20050412) and #6 (48UR20060608) showed low MAD values. Cruise #3 and #6 had MADs of 5.4 and 6.9 µmol/kg, respectively, indicating lower precision.
- Algéro-Provençal region (DF1): ten cruises sampled this subregion. Cruise #24 (48QL20171023) showed the highest MAD (7.5µmol/kg) and the highest median, but was based on only two profiles which likely explains the high uncertainty. Cruise #3 again exhibited an anomalously high median (197.6 µmol/kg), and cruise #6 (48UR20060608) had a notably high MAD of 4.2 µmol/kg.

- Algerian basin (DS3): ten cruises generally agreed well (MAD: 1.8-4.1 µmol/kg). Cruise #22 (48UR20131015, caried out in 2013) had elevated oxygen concentrations that may reflect real increases in deep oxygen. In contrast, cruise #3 (48UR20050412, carried out in 2005), showed a regionally high median, suggesting possible data quality issues.
- Northern Tyrrhenian (DT1): among 14 cruises, MAD ranged from 1 to 4.5 µmol/kg. Cruises #3 (48UR20050412) and #222 (48QL20151123) had higher MAD values, with cruise #3 also showing a high median, while cruise #2 (48UR20041006) recorded the lowest deep oxygen concentrations.
- Southern Tyrrhenian (DT3): the most frequently sampled region, with 20 cruises. MAD ranged from 0.1 and 5.3 µmol/kg. Elevated MAD values were observed for cruises #2 (48UR20041006), #3 (48UR20050412), #5 (48UR20051116), #6 (48UR20060608), #10 (48UR20080318), and #24 (48QL20171023), suggesting increased noise in the profiles.
- Sardinia Channel (DI1): fifteen cruises generally had consistent medians, though MAD values were higher (3.5 to 6.5 µmol/kg). Recent cruises, particularly cruise #24 (48QL20171023), showed the highest median (202.2 ±6.3 µmol/kg), significantly higher than earlier cruises, possibly indicating calibration issues.

Following an approach adapted from Olsen et al. (2016), large MAD values, combined with anomalous medians and limited spatial coverage were used to identify cruises with low internal precision and potential systematic biases:

- Cruise #3 (48UR20050412), recurring multiple subregions, consistently showed high MAD or biased medians.
- Cruise #6 (48UR20060608) displayed unusually high medians (e.g., in DF3) and high MAD in DS2 and DT3.
- Cruise #24 (48QL20171023) (in DS3 and DT1) and cruise #22 (48UR20131015) exhibited elevated deep oxygen values and large MAD values, raising concerns about data quality or calibration.
- Cruise #2 (48UR20041006) (in DT1 and DT3) and cruise #5 (48UR20051116) showed both low median and high MAD a values, pointing to possible systematic error.

To support the regional assessment of data quality, a summary table (Table 3) compiles the number of cruises per subregion, highlights those with high MAD, and identifies cruises exhibiting anomalous median values. This table facilitates the identification of cruises with potential CTD-O_2 bias issues and helps assess the overall initial internal consistency of the CTD-O_2 dataset across the WMED.

Table 3. Summary of CTD-O₂ Quality Control Results by Subregion

Subregion	Nb Cruises	Cruises with high MAD	Cruises with biased median	Notes
DF3 – Ligurian Sea	5	#3, #21	#3 (low), #6 (high)	Cruise #6 shows high values despite low MAD – potential calibration issue
DS2 – Balearic Sea	6	#3, #6	–	Both cruises show poor precision (high MAD)
DF1 – Algéro-Provençal	10	#24, #6	#3 (high), #24 (high)	#24 based on only 2 profiles; #6 and #3 raise concerns
DS3 – Algerian Basin	10	–	#3 (high), #22 (high)	#22 might reflect real signal; #3 likely biased
DT1 – Northern Tyrrhenian	14	#3, #222	#3 (high), #2 (low)	#2 and #3 indicate potential systematic errors
DT3 – Southern Tyrrhenian	20	#2, #3, #5, #6, #10, #24	#2 (low)	Frequent high MAD suggests noise or calibration issues
DI1 – Sardinia Channel	15	Most, esp. #24	#24 (high)	#24 significantly higher than earlier cruises – possible calibration bias

(a)   **(b)**
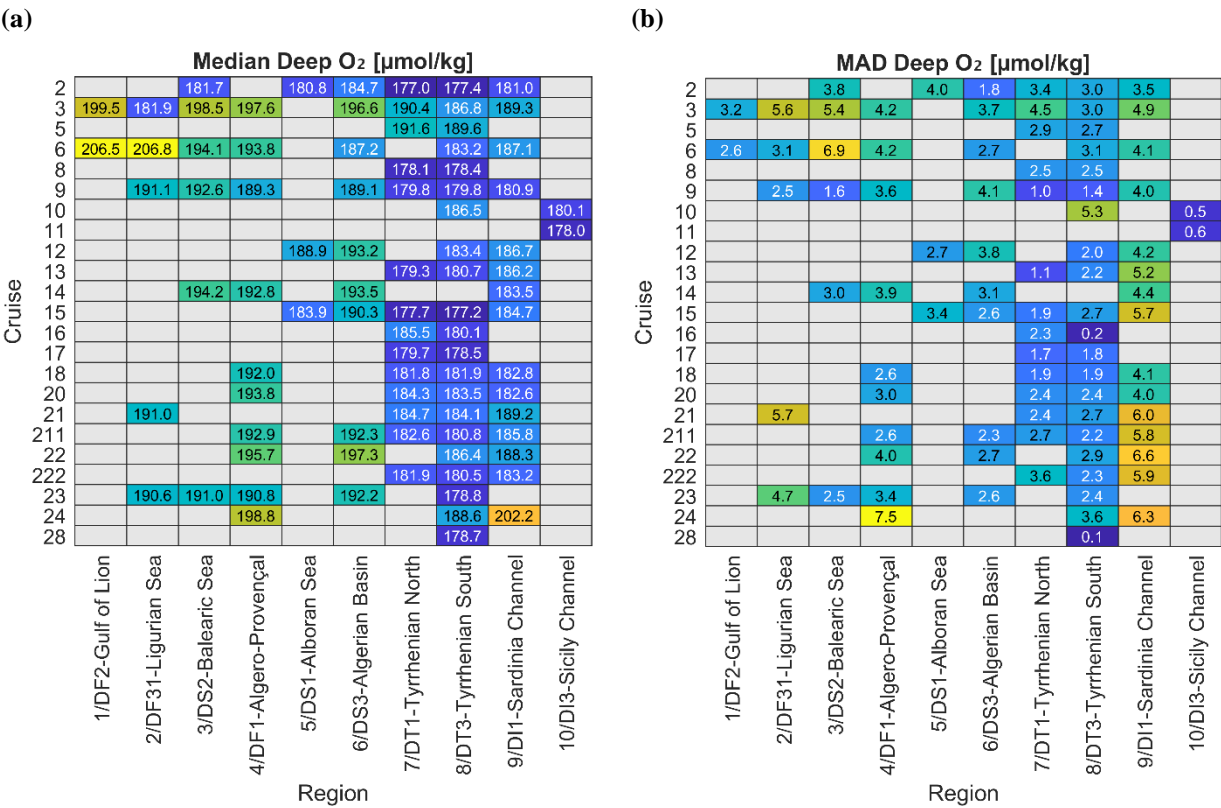
Figure 6. Median and median absolute deviation (MAD) of CTD-O₂WMED flagged as good data deeper than 800 dbar. Heatmaps show (a) the median and (b) MAD values, organized by cruise ID (rows) (Table 1) and geographic subregion (Figure 5) (columns). Grey cells indicate missing data. Theses metrics enable intercomparison of deep oxygen distribution and data quality across the CTD-O₂WMED dataset (Table S3). Color gradient: Blue to Green to Yellow indicate low to high values.

3.4 Secondary quality control procedure

The secondary quality control (2nd QC) procedure involves comparing the CTD-O₂ data from CNR cruises (Table 1) with selected reference cruises (Table 2). These reference datasets are assumed to be accurate and precise, with low temporal variability particularly in the deep ocean. However, this assumption may not fully hold for recent

cruises due to strong spatial gradients and potential long-term trends in dissolved oxygen concentrations in the Mediterranean Sea.

Global synthesis efforts like GLODAP (www.glodap.info) (Key et al., 2004; Olsen et al., 2016, 2019; Lauvset et al., 2024) and CARINA (Key et al., 2010) typically adopt a 1% threshold in crossover analysis to identify measurement biases and ensure inter-cruise consistency for oxygen. However, applying this same threshold to the Mediterranean may not be appropriate due to its unique oceanographic variability. Here, we assess the validity of reference cruise data, determine appropriate consistency thresholds, and identify the most temporally stable depth range for the crossover analysis in the WMED.

3.4.1. Threshold limit for dissolved oxygen data in the WMED

GLODAP applies a consistency or threshold limit for O_2 data of 1% as commented previously. However, given the natural variability in the Mediterranean Sea deep waters, we first assessed the appropriate threshold for crossover analysis by comparing reference cruise data in two different regions, DS3 and DT1, two subregions with distinct deep-water dynamics. Winkler O_2 data from these reference cruises were interpolated to standard pressure intervals (0 - 3600 dbar) using a piecewise cubic Hermite interpolation to obtain station profiles. Then, for each cruise and region, we calculated mean profiles (Figure 7).

The Algerian basin (region DS3, Figure 7a) exhibited clear temporal variability. Deep O_2 values (> 1500 dbar) in cruises from 2018 to 2022 were 4-5 µmol/kg lower than those from earlier years – a 2-4% deviation. These differences likely reflect reduced deep convection in recent years (Li and Tanhua, 2020; Schneider et al., 2014), consistent with long-term observations and tracer-based studies.

Reference cruises 06M220180302 and 11BG20220517 in DS3 consistently report 2-4% lower deep O_2 levels compared to earlier cruises (e.g., 06MT20110405, 29AH20140426, 29AJ20160818) (See Figure S2), corroborating the results of Gregoire et al. (2023) and L. Coppola (pers. comm.), who linked the 2022 anomaly to weakened deep convection. In contrast, the Tyrrhenian Sea (region DT1, Figure 7b), O_2 profiles between 800 and 2500 dbar were remarkably consistent across cruises, suggesting more temporally stable conditions in deep waters. This is consistent with the region's known ventilation regime, which is dominated by lateral advection and double-diffusion rather than convection (Durante et., 2009). Small interannual variations, such as the modest O_2 increases observed in 2007 and 2016, may reflect episodic ventilation events. These may also influence the development of a well-defined tracer minimum zone (TMZ) in the Tyrrhenian Sea (Li and Tanhua, 2020).

Figure 7c-d illustrate the variability of deep ocean O_2 concentrations in the WMED regions across cruises and support adopting a 2% threshold to study the consistency of the CTD-O_2WMED dataset in all subregions (Figure S1-S2).

(a) DS3- Algerian basin
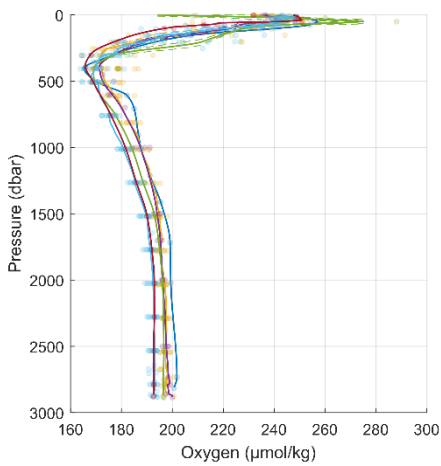
(b) DT1- Tyrrhenian Sea
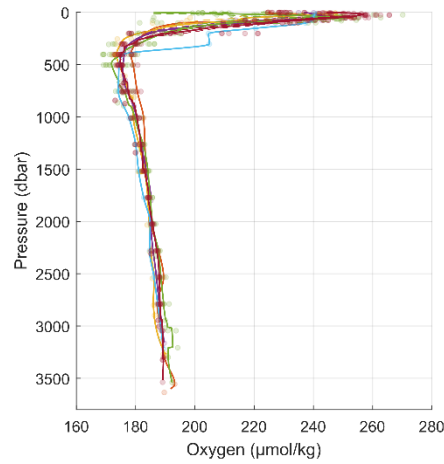
(c)
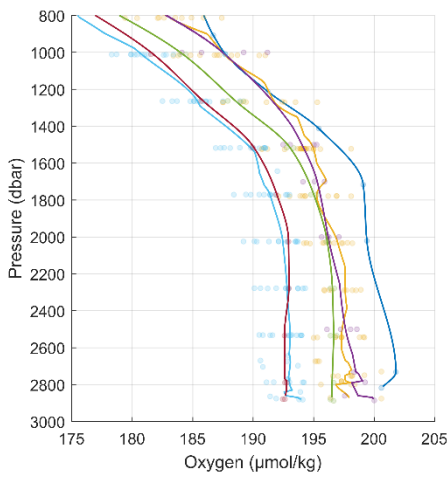
(d)
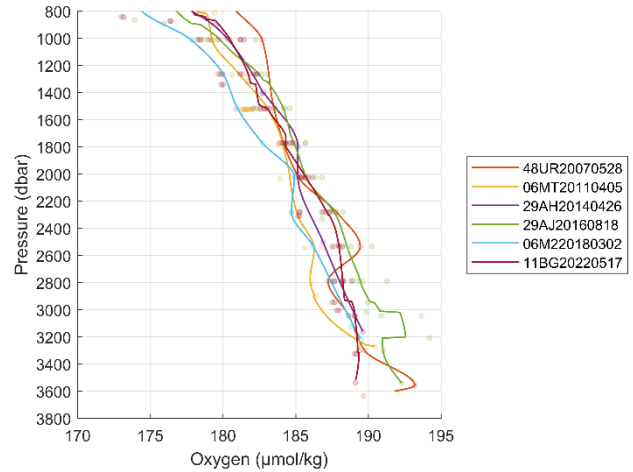
Figure 7. Average vertical profiles of dissolved oxygen in (a) the Algerian basin (region DS3) and (b) the Tyrrhenian Sea (region DT1). Panels (c) and (d) provide a zoomed view of the deep layers below 800 dbar. Colored dots represent discrete Winkler oxygen measurements, color-coded by cruise, while the solid-colored lines indicate cruise-specific mean profiles.

3.4.2. Defining a pressure range for the crossover analysis

The crossover results are evaluated in the water column region with the lowest temporal variability and lowest vertical gradient in terms of depth, density and/or potential temperature. Given the temporal changes in the Mediterranean Sea and particularly the WMED, we need to define our reference layer to evaluate the crossover results between cruises. Therefore, using the reference cruise O_2 data to determine the most stable depth range for crossover calculations, we computed pairwise ratios of mean profile O_2 values between the target reference cruise and other reference cruises in the subregion (e.g., A/B = 06MT20011018 / other reference cruises).

Results are shown in Figure 8 and Supplementary Figures S1-S2. As an overview, the results in Figure 8 clearly show that the deep and bottom waters in the WMED, below 2000 dbar, are not suitable to use as the most stable and reference layer, since here the data are sparse and natural variability increases.

 Below 800 db, in the Algerian basin (region DS3, Figure S2), 29.7% of pairwise ratios fall within 1%, 60.5% within 2%, while 39% exceed the 2% threshold – indicating greater variability. In the Tyrrhenian Sea (region DT1, Figure S1), 71.7% of ratios fall within 1%, and 98.7% within 2% – confirming greater stability.

336 The 800 – 2000 dbar range emerges as the most stable layer across cruises and regions and is selected as the

337 reference one to evaluate the crossover analysis results. This layer corresponds with the TMZ described by Li and

338 Tanhua (2020) and is less affected by long-term ventilation trends.

339

340
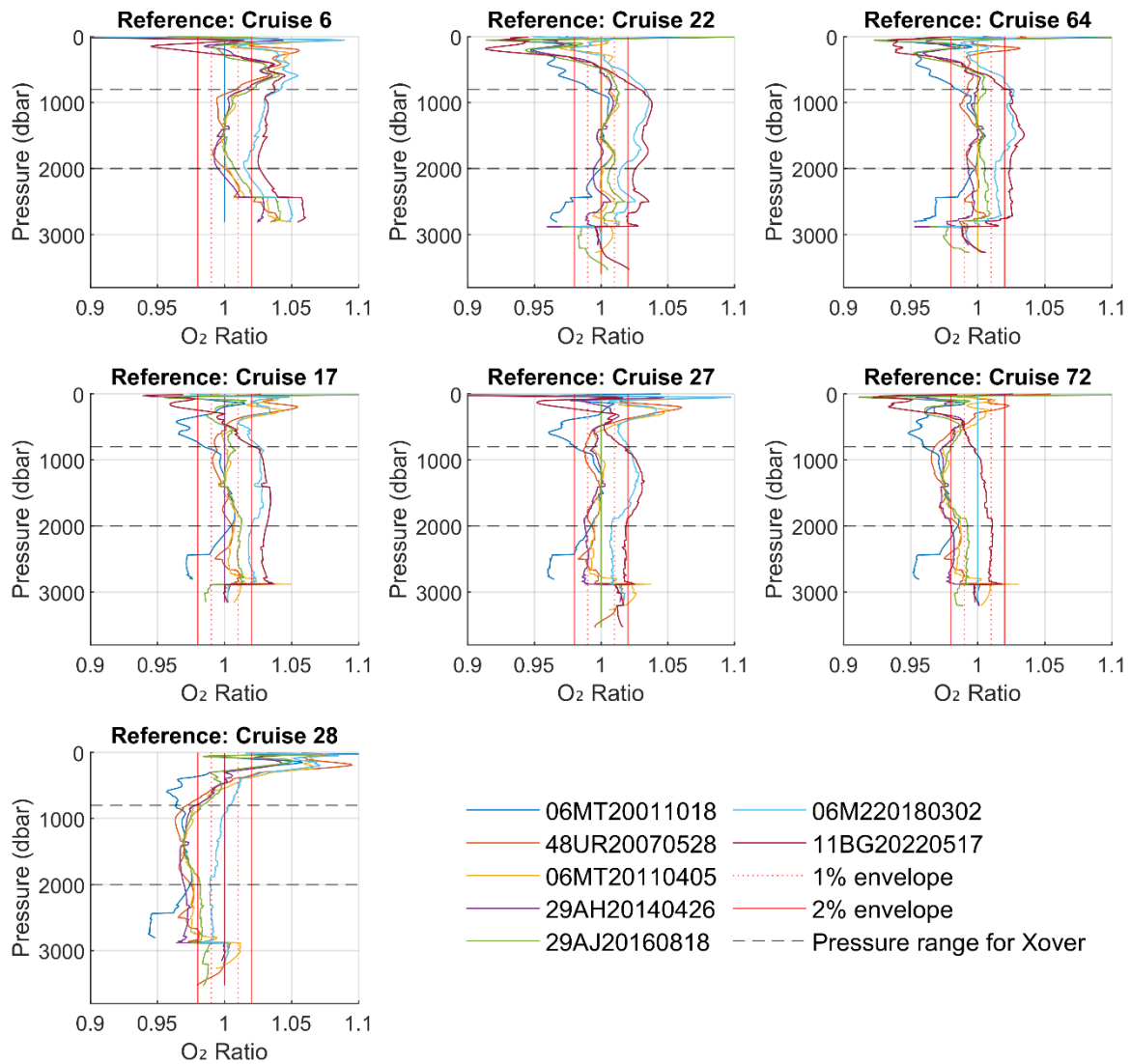
Figure 8. Vertical distribution of the ratio between mean dissolved oxygen profiles from Winkler discrete measurements for the reference cruises, each tested reference cruise (indicated at the top of each subplot) and the other reference cruises (listed in the legend box). The solid red vertical line marks the ±2% threshold limit, while the dashed red line indicates the ±1% threshold. Similar composite figures for subregions DT1 and DS3 are provided in the Supplementary Material (Figures S1 and S2, respectively), focusing on the 800-2000 dbar depth range.

3.4.3. Crossover analysis

348 The crossover analysis was performed following Johnson et al. (2001) and Tanhua et al. (2011), taking advantage

349 of the software tool provided in Lauvset and Tanhua (2015). CTD-O_2WMED cruises were compared with

350 reference cruises by pairing stations within a 2° radius (~222 km). Interpolated profiles from each new cruise from

351 CTD-O_2WMED (C1) were compared to those from the reference cruise (C2) within this distance. Each crossover

352 comprises a minimum of three stations from each cruise where CTD-O_2 profiles were interpolated to standard

density levels (sigma4) using Hermite interpolation. Using sigma4 as the vertical coordinate assures the comparison is made in the same water masses, thereby mitigating biases associated with variations in salinity. Mean difference profiles were computed at each crossover as the mean of different station pair differences, thus, one station in cruise C1 is compared to all stations in cruise C2, resulting in multiple mean difference profiles to finally calculate for each crossover pair the corresponding weighted mean and standard deviation profile, which are finally used to determine the weighted offset and standard deviation for the crossover pair. The weighting applied to the profiles is based on their variability, giving higher importance to parts of the profiles with lower variability (adapted from Tanhua et al., 2010, 2015). Figure 9 illustrates an example of a crossover pair and the corresponding offset between a CNR cruise and a reference cruise The number of crossover stations is critical because low sample sizes increase uncertainty: as illustrated in Figure 9a, 30 stations from C1 and 14 from C2 were compared. Additionally, while the number of crossover pairs is significant, the Mediterranean Sea has a limited number of reference cruises available. All calculated offsets for each cruise were therefore examined to determine the presence of any likely biases in the measurements.

In addition to the typical crossover analysis, we performed a regional crossover analysis using a simple modified clustering approach based on predefined WMED subregions (Table S2). Regional clusters included the Tyrrhenian Sea (DT1 and DT3), the Algerian basin (DS3 and DF1), and the Alboran Sea (DS1). Clusters were set manually by defining each subregion subsets following the geographical limits in table S2. This approach minimizes the impact of regional hydrographic differences.

3.4.4. Correction factors and final product consistency evaluation

For each cruise a set of offsets was obtained after the crossover analysis, and the corresponding inverse values are the Correction Factors (CF) which set the basis to obtain the final cruise CF for CTD-O_2 if needed. We applied a conservative approach: among the regional offsets, the CF closest to 1 (i.e., lowest absolute deviation) was selected (Table 3). This minimizes changes to the original data while improving internal consistency.

After applying the cruise CF, the final step involves evaluating the overall internal consistency of the CTD-O_2WMED dataset. This is done using the weighted mean (*WM*) which is calculated from the absolute offsets (*D*) across all crossovers (*L*) after adjustment, weighted by the corresponding standard deviation (σ), following the approach described by Tanhua et al. (2009) and Belgacem et al. (2020).

$$WM = \frac{\sum_{i=1}^{L} D(i)/(\sigma(i))^2}{\sum_{i=1}^{L} 1/(\sigma(i))^2}$$

This assessment provides a quantitative measure of the internal coherence of the final data product, following earlier studies (Hoppema et al., 2009; Sabine et al., 2010; Tanhua et al., 2009). It is important to note that the evaluation is based on offsets relative to a selected reference dataset, under the assumption that these reference cruise data represent the trueness state of dissolved oxygen in the WMED.
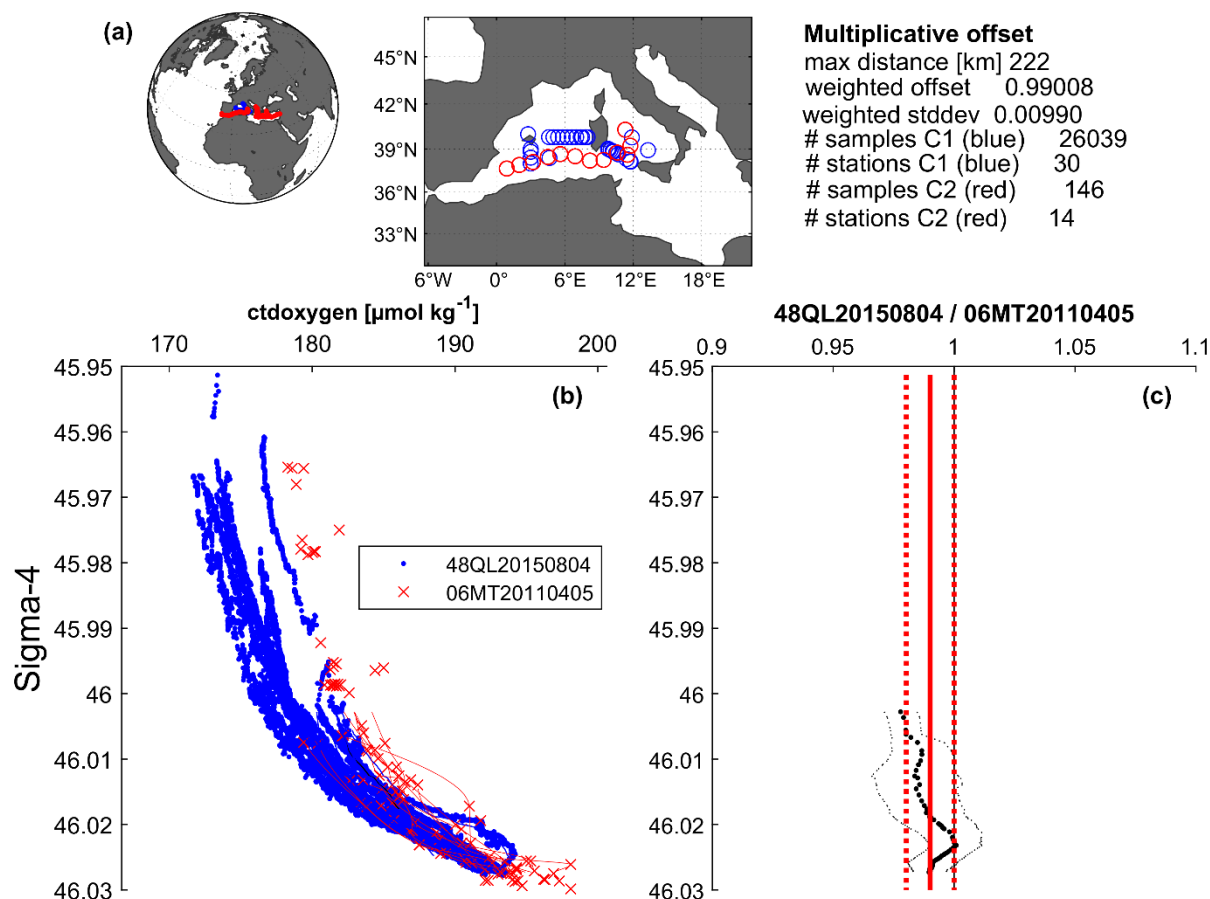
Figure 9. Example of a crossover pair analysis to obtain the offset ratio (multiplicative offset) in dissolved oxygen between cruise 48QL20150804 and the reference cruise 06MT20110405. (a) Spatial distribution of stations included in the crossover analysis: target cruise (blue) and reference cruise (red), with accompanying summary statistics. (b) Vertical profiles with sigma4 of dissolved oxygen (µmol/kg) from both cruises within a 2° radius and the 800 – 2000 dbar depth range. (c) Differences in dissolved oxygen between the two cruises: thick black dotted line shows the mean offset profile and the thin black dotted lines represent the standard deviation; the solid red line indicates the weighted average offset, and red dotted lines show the weighted standard deviation, values that are showed in the summary statistics in (a).

4 Secondary quality control results, correction factors to improve the CTD-O₂ WMED dataset

4.1 Overview of the secondary quality control results and impact on the CTD-O₂ WMED dataset

This section describes the obtained crossover results and discusses the correction factor and the final adjustments applied, if needed, to each CNR WMED cruise, to finally probe the increased consistency of the CTD-O₂ WMED data product released. Each crossover result was evaluated, somehow subjectively, considering its quality, which would depend on the number of available stations, the calculated standard deviation of the offset, the depth range covered and the regional variability. A total of 265 crossover results for each cruise including regional clusters were carefully inspected and only the appropriate ones; following the conservative approach; were considered to obtain the correction factors (Figure 10). The final correction factors applied are summarized in Table 4 and only applied when the offset exceeded the ±2% threshold limit. Overall, only a few cruises exhibited deviations outside the ±2% limit, and thus required adjustments (Figure 10). The analysis indicated that deep oxygen values from cruises #2 (48UR20041006), #8 (48UR20060928), #211 (48UR20130604) and #222 (48QL20151123) required upward correction to align with the reference dataset. Conversely, cruises #3 (48UR20050412), #5 (48UR20051116), and #24

408   (48QL20171023) showed slightly higher values compared to their respective reference and were adjusted

409   downward. Fourteen cruises did not require any correction, as their values were consistent with the reference

410   dataset. Cruises #25 (48DP20180918), #27 (48DP20221015), and #28 (48DP20230324) were excluded from the

411   crossover analysis due to an insufficient number of deep stations below 800 dbar, but their data remain part of the

412   final dataset. The reader is encouraged to compare the descriptions with the corresponding plots in Figure 10 and

413   the crossover summary figures in the Supplementary Material (Figures S3 to S9).

414   After applying the correction factors listed in Table 4, the offsets were recalculated to validate the adjustments. As

415   shown in Figure 10, the corrected values (in blue) reduced the recalculated offsets and improved consistency. To

416   assess the overall consistency of the adjusted CTD-O_2WMED dataset, we computed the WM of the crossover

417   offsets after adjustments (Figure 11). The internal consistency of the final CTD-O_2WMED dataset was estimated

418   at 0.998. These adjustments reduced potential biases linked to errors related to methodological discrepancies,

419   resulting in improved coherence across the dataset.

420
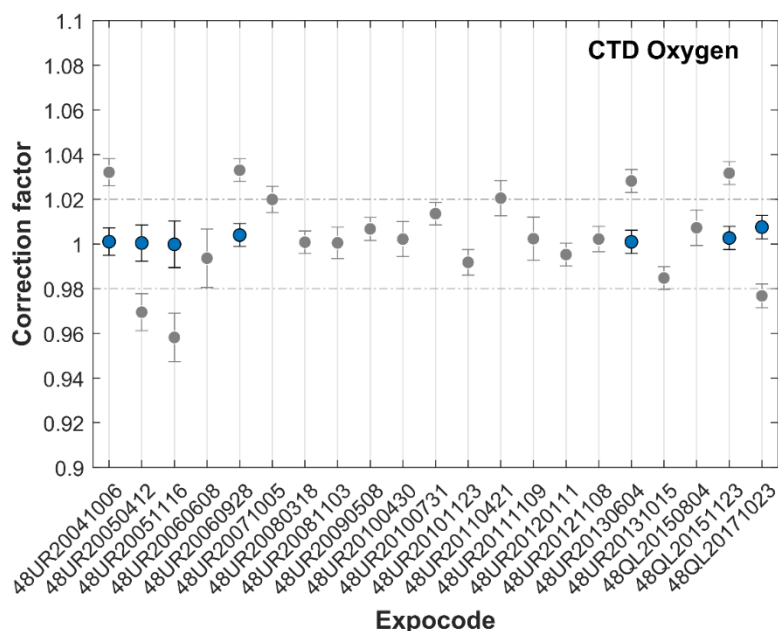
421   **Figure 10**. Results of the crossover analysis for CTD dissolved oxygen, showing the recommended correction
422   factors before (grey) and after (blue) adjustment (i.e., after applying the correction factor). Error bars represent the
423   standard deviation of the absolute weighted offset. Corrections indicate the multiplicative factor to be applied to
424   the original CTD oxygen data (see Table 4). The dashed line marks the ±2% threshold limit of adjustment.

425

426

427

428

429

430

431

432 **Table 4**. Summary of the recommended multiplicative correction factors for the CTD-O2WMED cruises derived
433 from the 2nd QC procedure.

Cruise ID	EXPOCODE	Ajustements
2	48UR20041006	1.032
3	48UR20050412	0.97
5	48UR20051116	0.96
6	48UR20060608	-
8	48UR20060928	1.03
9	48UR20071005	-
10	48UR20080318	-
11 + 12ᵃ	48UR20080905 + 48UR20081103	-
13	48UR20090508	-
14	48UR20100430	-
15	48UR20100731	-
16	48UR20101123	-
17	48UR20110421	-
18	48UR20111109	-
20	48UR20120111	-
21	48UR20121108	-
211	48UR20130604	1.028
22	48UR20131015	_
222	48QL20151123	1.03
23	48QL20150804	-
24	48QL20171023	0.97

434 [a] Cruise #11 and cruise #12 were merged in the 2nd QC.
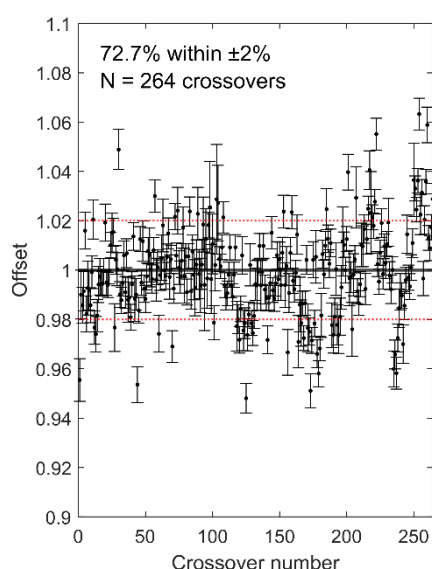
436 **Figure 11.** Crossover results showing the weighted mean offset and standard deviation for the CTD-O₂WMED
437 cruises after applying the correction factors. The dashed red line marks the ±2% threshold.

438

4.2 Detailed description of each CNR WMED cruise corrected

440 This subsection provides a rationale for the proposed correction factors in Table 4. It includes interpretations of
441 significant offsets, even in cases where no final correction was applied but poor data quality was observed. Cruises
442 not mentioned below were found to be consistent with the reference data and required no further review.

443   -   Cruise#2 (48UR20041006): Two crossovers were found in the Alboran Sea, five in the Algerian basin,
444   and four in the Tyrrhenian Sea. A consistent mean offset of 0.96±0.005 across all regions suggests CTD-
445   O_2 values were ~4% lower than the reference cruises (Figure 12). This is also supported by high residuals
446   between Winkler and sensor data (>2 µmol/kg, Figure 3) and by the unusually low regional deep averages
447   (Figure 6). Given that deep WMED ventilation prior to 2004 was still stable, a 3.2% increase. An
448   adjustment of 1.032 is applied.

449
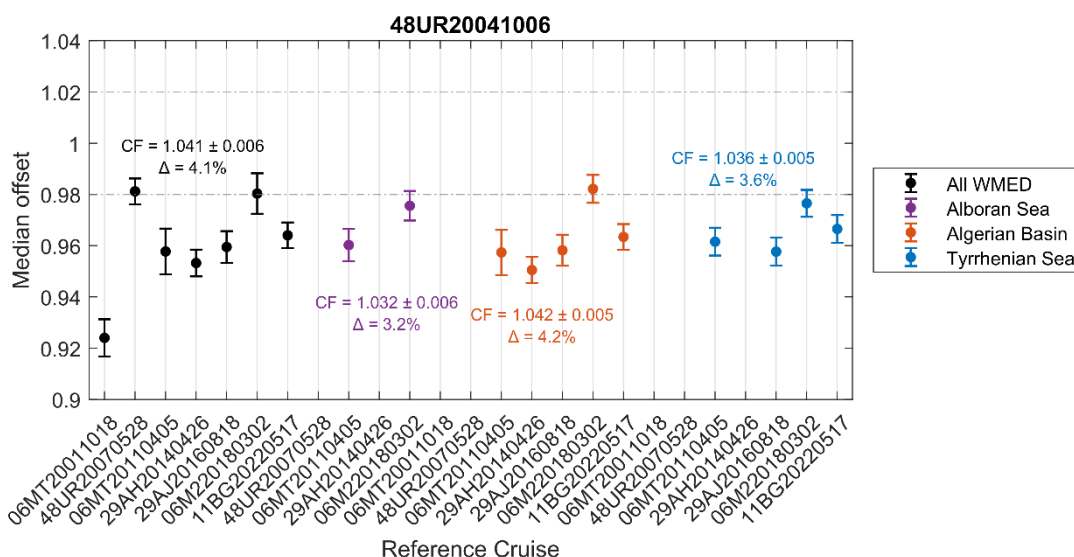
450   **Figure 12.** Summary of CTD-O_2 crossover results for cruise #2 (48UR20041006) relative to the reference cruises
451   showed along the x-axis arranged chronologically. Dashed grey lines indicate the ±2% threshold. Black dots with
452   error bars represent the weighted mean offsets and corresponding weighted standard deviation. Colored markers
453   denote the subregions: purple for the Alboran Sea, orange for the Algerian basin, and blue for the Tyrrhenian Sea.
454   Annotated within the figure are the correction factor, standard deviation, and percentage change of the median
455   offsets for each subregion.

456

457   -   Cruise #3 (48UR20050412): this cruise has five crossovers in the Algerian basin and four in the
458   Tyrrhenian Sea clearly indicating the need for a downward adjustment. As pointed out in section 3.3, this
459   cruise could be of low precision compared to cruises conducted in the same regions. Based on the
460   agreement between the offsets in both subregions (Figure 13), and despite one reference cruise in 2001
461   suggested agreement (but it involved only three stations, therefore it is not robust). An overall offset of
462   1.03±0.008 was found, supporting an adjustment of 0.97 (- 3%).

463
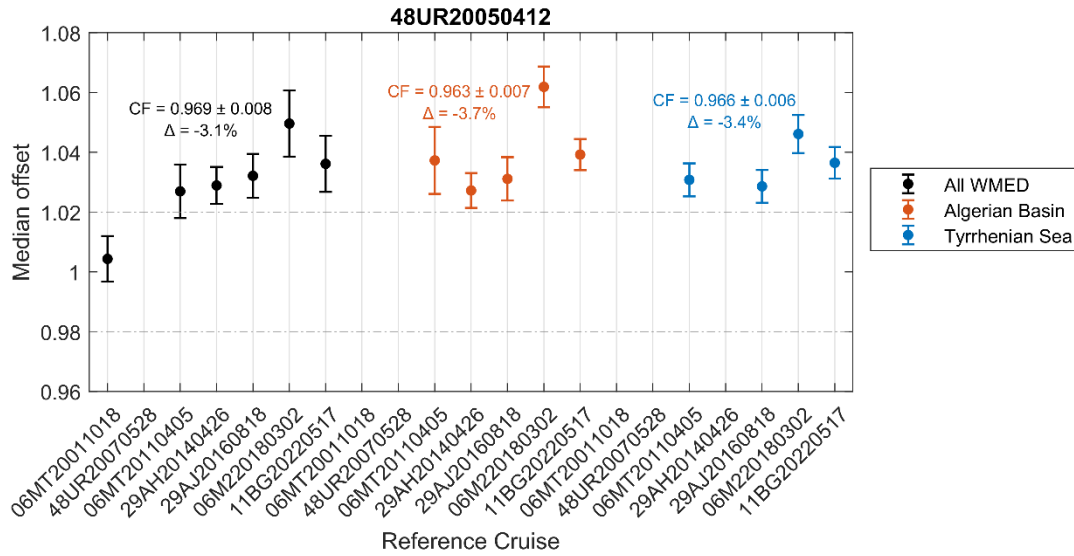
Figure 13. Same as Figure 12 but for cruise #3 (48UR20050412).

- Cruise #5 (48UR20051116): four crossovers in the Tyrrhenian Sea spanning the years 2011, 2016, 2018 and 2022 (Figure S3) showed good agreement (weighted standard deviation of 0.01), but a median weighted offset of 1.042±0.01. The suggested correction is ∼ 4% lower. The quite large discrepancy may indicate potential issues with the sensor (section 3.3, Table 3). An adjustment of 0.96 is applied.

- Cruise #6 (48UR20060608): five crossovers in the Algerian basin and four in the Tyrrhenian Sea (Figure S.4). While offsets seem to increase over time, seven of nine crossovers were lower than ±2%. The Tyrrhenian Sea, a quite stable region for deep waters, showed low variability (weighted standard deviation of 0.005), indicating a good precision and good agreement between crossovers. The Algerian basin was more variable and represented the direct effect of the Gulf on Lion (where deep-water convection may occur). Here, the weighted standard deviation was higher (∼ 0.01), persistent in all references except for the 2022 reference. Given the lack of consistency between subregions and trends similar to reference profiles (Figure 7c), no adjustment is applied.

- Cruise #8 (48UR20060928): four crossovers in the Tyrrhenian Sea showed good agreement (weighted standard deviation of 0.005), with reference cruises 06MT20110405, 29AJ20160818, 06M220180302 and 11BG20220517 (Figure S5). Offsets were found to be between 0.96±0.005 and 0.97±0.005, and an increase of +3% is recommended. And adjustment of 1.03 is applied.

- Cruise #9 (48UR20071005): crossovers in both the Algerian basin (5) and Tyrrhenian Sea (4) showed consistent offsets of 0.97±0.01-0.98±0.005, indicative of the good precision of the data. The largest offset (0.95±0.005) occurred with reference cruise 06MT20011018 (Figure 14), likely due to limited station coverage. Both subregions show a consistent deviation about +2% but as all values remain within the ±2% limit no adjustment is recommended.
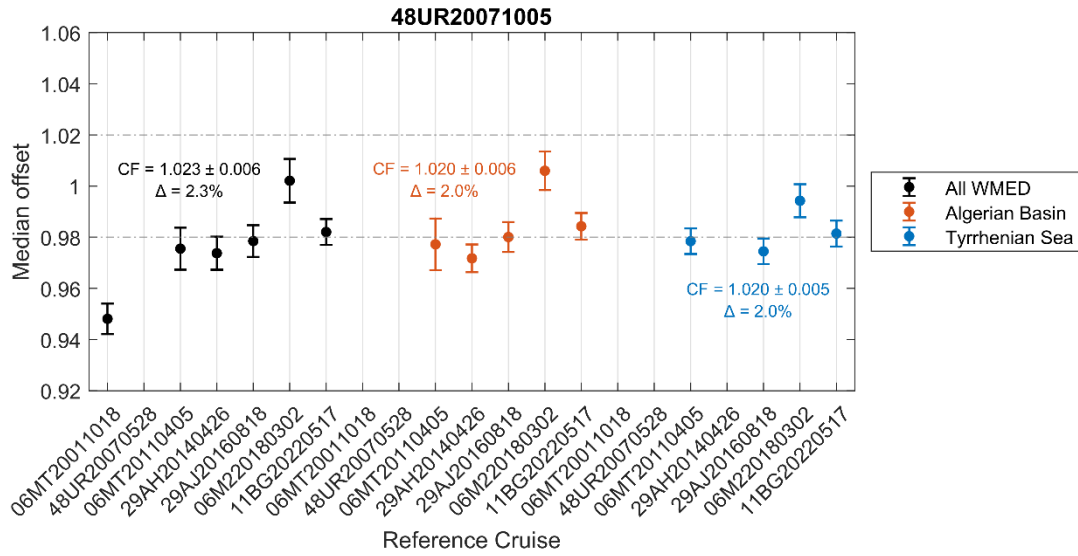
Figure 14. Same as Figure 12 but for cruise #9 (48UR20071005).

- Cruise #15 (48UR20100731): two crossovers in the Alboran Sea with a median offset of 0.98±0.01, five crossovers in the Algerian basin with an offset of 0.98±0.005, and four crossovers in the Tyrrhenian Sea showing an offset of 0.97±0.005 (Figure S6). Following our conservative correction approach, the lowest observed percentage of change is 1.4% in the Algerian basin, suggesting a correction factor of 1.014, below the ±2% threshold limit. Therefore, no adjustment is applied.

- Cruise #211 (48UR20130604): the crossovers suggest a 6% increase in the Algerian basin and 2.8% in the Tyrrhenian Sea (Figure 15). Both median offsets indicate that oxygen data for this cruise are lower than the references, although data precision appears good. Despite the regional difference and following our conservative approach, we recommend applying an increase of +2.8%, prioritizing the smaller offset to avoid overcorrection. An adjustment of 1.028 is applied.

- Cruise #22 (48UR20131015): this cruise was carried out in the same year as cruise #211 (48UR20130604), but shows smaller offsets in both regions (Algerian basin and Tyrrhenian Sea) (Figure S7), suggesting its oxygen values are higher than the references and might require a small downward correction of -1.5%, that is within the ±2% limit. No adjustment is applied.

Figure 15. Same as Figure 12 but for cruise #211 (48UR20130604).

- Cruise #222 (48QL20151123): four crossovers in the Tyrrhenian Sea, spanning multiple years (Figure S8), indicated a consistent underestimation of CTD-O_2 data (offset 0.97±0.005). The data exhibit good precision, with a weighted standard deviation of 0.005. An of 3% is recommended. A final adjustment of 1.03 is applied.

- Cruise #24 (48QL20171023): four crossovers in the Tyrrhenian Sea (Figure S9) show CTD-O_2 values slightly higher than the reference cruises. The median offset suggests a decrease indicating a correction factor of 0.97. Precision remains high with weighted standard deviation of 0.005. Additionally, as shown in Figure 3, the residuals between Winkler and sensor measurements for this cruise was classified as poor, supporting the need for an adjustment of 0.97.

To resume, the CTD-O2WMED original version includes all cruises that has passed the first levels of quality checks, but has not yet been corrected through crossover analysis (i.e., secondary quality control), so no adjustments were applied the original version. However, the adjusted version of the dataset CTD-O2WMED-adjusted builds upon the original dataset by incorporating the secondary quality control adjustments.

5   Summary and conclusions

This study aimed to evaluate and enhance the consistency of a collection of CTD-O_2 measurements of 25 cruises in the WMED with a relevant CNR Italian participation. A 1st quality control was applied followed by a secondary quality control procedure based on crossover analysis was adapted to the specificizes of the dataset and the WMED: the threshold limit was increased from 1% to 2% recognizing the limitations in terms of accuracy and precision of our dataset and the known temporal variability in some WMED basins; and we determined it is more appropriate to study the consistency of CTD-O_2 data in the 800-2000 dbar layer rather than the deep and bottom waters which are much more variable. The methodology developed here provides a robust and transferable framework for quality control in regions with similarly complex hydrography.

The 2nd QC procedure obtained a total of 265 crossover comparisons between the CTD-O$_2$ data and Winkler measurements from a selection of reference cruises following GO-SHIP procedures, with a higher precision and accuracy. While the majority of checked CTD-O$_2$ cruise data fell within the ±2% limit, a limited number showed systematic offsets that warranted correction. Adjustments were applied conservatively—only when deviations exceeded the defined threshold and using the smallest possible correction factor. Adjustments were recommended for seven cruises. Although these cruises are categorized as moderate in quality, they are retained in the final dataset as adjusted data. A few cruises (#25 (48DP20180918), #27 (48DP20221015), and #28 (48DP20230324)) were excluded from the crossover analysis due to insufficient deep profiles but remain part of the final dataset. The corrections led to a measurable improvement in the internal consistency of CTD-O$_2$ data among cruises, as demonstrated by the weighted mean global offset of 0.998 calculated from post-adjustment crossover analysis.

The CTD-O$_2$WMED original and corrected dataset is openly accessible to the scientific community through open access repositories. Our product, despite limitations in temporal coverage, will substantially increase the availability and reliability of dissolved oxygen data for long-term studies in the WMED. It builds upon and complements earlier efforts in the region (Schneider et al., 2014; Coppola et al., 2017; Macías et al., 2018b; Mavropoulou et al., 2020; Li and Tanhua, 2020; Cossarini et al., 2021; Friedland et al., 2021; Ulses et al., 2021; Belgacem et al., 2019, 2020). Recent advances in numerical modeling (Reale et al., 2021), machine learning (Fourrier et al., 2022), and autonomous platforms such as BGC-Argo floats and gliders in the WMED demand measurements to validate their results. The CTD-O$_2$WMED dataset, in synergy with these emerging observation systems, provides a valuable foundation for assessing changes in the regional oxygen budget and it will support ongoing efforts to understand the WMED's response to climate-driven oceanographic changes and improve future projections.

6   Data availability

The CTD-O2WMED dataset (Belgacem et al., 2025) is available at PANGAEA (https://doi.org/10.1594/PANGAEA.982858)

Table 5 shows the variables included in the dataset, which is composed in two parts:

- CTDO2_WMED_2004_2023_original: the first includes the aggregation of cruise data prior to correction, which has undergone calibration and first-level quality check:
- CTDO2_WMED_2004_2023_adjusted: the second contains the adjusted data product, incorporating the final adjustments from the secondary quality control procedure.

The CTD-O$_2$WMED is complementary to the data product CNR-DIN-WMED available https://doi.org/10.1594/PANGAEA.904172.

No special software is required to access the data. Note that data from the reference cruises used for crossover analysis are not included in the final product (see Table 6).

562 **Table 5.** List of parameters for the CTD-O2WMED dataset for both original and adjusted versions.

Data Product Parameter Name	Parameter Name	Units
EXPOCODE	expedition code	
CRUISE	cruise number	
STATION	profile number	
CRUISE_ID	cruise id	
DAY	day	
MONTH	month	
YEAR	year	
LONGITUDE	longitude	decimal degrees [DEGREES_EAST]
LATITUDE	latitude	decimal degrees [DEGRES_NORTH]
CTDPRS	CTD pressure	decibars [DBAR]
DEPTH	depth	meters [M]
CTDSAL	CTD salinity	[PSS-78]
CTDSAL_FLAG_W	CTD salinity flag	
CTDTMP	CTD temperature	degrees C [ITS-90]
CTDOXY	CTD oxygen	micromole/kg [UMOL/KG]
CTDOXY_FLAG_W	CTD oxygen flag	

563

564 **Table 6**. Reference dataset availability (Last access June 2025)

Reference cruise expocode	Availability
06MT20011018	https://cchdo.ucsd.edu/cruise/06MT20011018
48UR20070528	https://www.ncei.noaa.gov/archive/archive-management-system/OAS/bin/prd/jquery/accession/details/218462
06MT20110405	https://cchdo.ucsd.edu/cruise/06MT20110405
29AH20140426	https://catalog.data.gov/dataset/dissolved-inorganic-carbon-dic-total-alkalinity-ph-on-total-scale-chlorofluorocarbon-12-cfc-12-3
29AJ20160818	https://cchdo.ucsd.edu/cruise/29AJ20160818
06M220180302	https://cchdo.ucsd.edu/cruise/06M220180302
11BG20220517	https://cchdo.ucsd. edu/cruise/11BG20220517

565

Authors contributions

567 MB ran the analysis and wrote the manuscript. KS contributed to writing the manuscript. MA, SKL contributed
568 to the analysis. JC contributed to specific parts of the manuscript. MiB and SS coordinated the technical aspects
569 of most of the cruises. CC and TC assisted some of the chemical analysis.

Competing interest

571 The authors declare that they have no conflict of interest.

Acknowledgements

573 M. Belgacem's postdoctoral fellowship was supported by the EuroGO-SHIP project, funded by the European
574 Union under Grant agreement No. 101094690. The data have been collected within the framework of several
575 European projects, e.g. KM3NeT, EU GA no. 011937; SESAME, EU GA no. GOCE-036949; PERSEUS, EU GA
576 no. 287600; OCEAN-CERTAIN, EU GA no. 603773; COMMON SENSE, EU GA no. 228344; EUROFLEETS,
577 EU GA no. 228344; EUROFLEETS2, EU GA no. 312762; JERICO, EU GA no. 262584; and the Italian PRIN
578 2007 program "Tyrrhenian Seamounts ecosystems" and the Italian RITMARE flagship project, both funded by
579 the Italian Ministry of Education, University and Research.

580   We acknowledge the project PRIN PNRR 2022 - Prot. P2022LMCW2-SettorePE 10- "CLOSER: CLimate forcing
581   On   Adriatic   SEa   deoxygenation: A   multi-archive   Reconstruction   of   Sapropel   S1".   CUP
582   B53D23033660001 funded by the Italian Ministry of Education. M.A. acknowledges the PRX23/ 00051 project
583   funded by the Spanish Ministry of Science, Innovation and Universities from the "Salvador de Madariaga"
584   program. The authors are deeply indebted to the captains, crew, technical and research personnel involved in the
585   cruise data collection at sea, without them, this work would not have been possible. We also thank the Principal
586   Investigators of the cruises (Stefano Cozzi, Gabriella Cerrati, Stefano Aliani, Mario Astraldi, Maurizo Azzaro,
587   Alberto Ribotti, Massimiliano Dibitetto, Gian Pietro Gasparini, Annalisa Griffa, Jeff Haun, Loïc Jullion, Gina La
588   Spada, Elena Mannini, Angelo Perilli and Chiara Santinelli).

589

590

591

592

593

594

595

596

597

598

599

600

601

602

603

604

605

606

References

Álvarez, M., Sanleón-Bartolomé, H., Tanhua, T., Mintrop, L., Luchetta, A., Cantoni, C., Schroeder, K., and Civitarese, G.: The CO2 system in the Mediterranean Sea: a basin wide perspective, Ocean Sci., 10, 69–92, https://doi.org/10.5194/os-10-69-2014, 2014.

Álvarez, M., Catalá, T. S., Civitarese, G., Coppola, L., Hassoun, A. E. R., Ibello, V., Lazzari, P., Lefevre, D., Marcias, D., Santinelli, C., and Ulses, C: Chapter 11–Mediterranean Sea general biogeochemistry, Editor (s): Katrin Schroeder, Jacopo Chiggiato, Oceanography of the Mediterranean Sea, https://doi.org/10.1016/B978-0-12-823692-5.00004-2, 2022.

Álvarez, M., Velo, A., Tanhua, T., Key, R., Heuven, S. V.: Carbon, tracer and ancillary data in the medsea, CARIMED: an internally consistent data product for the Mediterranean Sea. Tech. Rep. 2019, Instituto Español de Oceanografía, 2019.

Belgacem, M., Chiggiato, J., Borghini, M., Pavoni, B., Cerrati, G., Acri, F; Cozzi, S., Ribotti, A., Álvarez, M., Lauvset, S. K., and Schroeder, K.: Quality controlled dataset of dissolved inorganic nutrients in the western Mediterranean Sea (2004– 2017) from R/V oceanographic cruises, PANGAEA [data set], https://doi.org/10.1594/PANGAEA.904172, 2019.

Belgacem, M., Chiggiato, J., Borghini, M., Pavoni, B., Cerrati, G., Acri, F., Cozzi, S., Ribotti, A., Álvarez, M., Lauvset, S. K., and Schroeder, K.: Dissolved inorganic nutrients in the western Mediterranean Sea (2004–2017), Earth Syst. Sci. Data, 12, 1985–2011, https://doi.org/10.5194/essd-12-1985-2020, 2020.

Belgacem, M., Schroeder, K., Lauvset, S. K., Álvarez, M., Chiggiato, J., Borghini, M., Cantoni, C., Ciuffardi, T., Sparnocchia, S.: CTD-O2WMED: Quality controlled dataset of CTD dissolved oxygen profiles in the Western Mediterranean Sea (2004-2023) from R/V oceanographic cruises [dataset]. PANGAEA, https://doi.pangaea.de/10.1594/PANGAEA.982858 (dataset in review)

Belgacem, M., Schroeder, K., Lauvset, S. K., Álvarez, M., Chiggiato, J., Borghini, M., Cantoni, C., Ciuffardi, T., Sparnocchia, S.: 2025: CTD-O2WMED: Quality controlled dataset of CTD dissolved oxygen profiles in the Western Mediterranean Sea (2004-2023) from R/V oceanographic cruises [dataset]. PANGAEA, https://doi.org/10.1594/PANGAEA.982858

Coppola, L., Prieur, L., Taupier-Letage, I., Estournel, C., Testor, P., Lefevre, D., Belamari, S., & Taillandier, V.: Observation of oxygen ventilation into deep waters through targeted deployment of multiple Argo-O₂ floats in the north-western Mediterranean Sea in 2013, *J. Geophys. Res.-Oceans*, 122, 6325–6341, https://doi.org/10.1002/2016JC012594, 2017.

Coppola, L., Legendre, L., Lefevre, D., Prieur, L., Taillandier, V., & Riquier, E. D. (2018). Seasonal and inter-annual variations of dissolved oxygen in the northwestern Mediterranean Sea (DYFAMED site). Progress in Oceanography, 162, 187-201, https://doi.org/10.1016/j.pocean.2018.03.001, 2018.

Cossarini, G., Feudale, L., Teruzzi, A., Bolzon, G., Coidessa, G., Solidoro, C., Di Biagio, V., Amadio, C., Lazzari, P., Brosich, A., and Salon, S.: High-resolution reanalysis of the Mediterranean Sea biogeochemistry (1999–2019), Front. Mar. Sci., 8, 741486, https://doi.org/10.3389/fmars.2021.741486, 2021.

Fichaut, M., Garcia, M. J., Giorgetti, A., Iona, A., Kuznetsov, A., Rixen, M., and Medar Group: MEDAR/MEDATLAS 2002: A Mediterranean and Black Sea database for operational oceanography, Elsevier Oceanography Series, 69, 645–648, https://doi.org/10.1016/S0422-9894(03)80107-1, 2003.

Fourrier, M., Coppola, L., Lebrato, M., Testor, P., Bosse, A., D'Ortenzio, F., Taillandier, V., de Madron, X. D., Mortier, L., Prieur, L., and Gatti, J.: Impact of intermittent convection in the northwestern Mediterranean Sea on oxygen content, nutrients, and the carbonate system, *J. Geophys. Res.-Oceans*, 127, e2022JC018615, https://doi.org/10.1029/2022JC018615, 2022.

Friedland, R., Macias, D., Cossarini, G., Daewel, U., Estournel, C., Garcia-Gorriz, E., Grizzetti, B., Grégoire, M., Gustafson, B., Kalaroni, S., Kerimoglu, O., Lazzari, P., Lenhart, H., Lessin, G., Maljutenko, I., Miladinova, S., Müller-Karulis, B., Neumann, T., Parn, O., Pätsch, J., Piroddi, C., Raudsepp, U., Schrum, C., Stegert, C., Stips, A., Tsiaras, K., Ulses, C., and Vandenbulcke, L.: Effects of nutrient management scenarios on marine eutrophication indicators: a pan-European, multi-model assessment in support of the Marine Strategy Framework Directive, Front. Mar. Sci., 8, 596126, https://doi.org/10.3389/fmars.2021.596126, 2021.

Garcia and Gordon (1992) "Oxygen solubility in seawater: Better fitting equations", Limnology & Oceanography, vol 37(6), p1307-1312.

Grasshoff, K., Ehrhardt, M., and Kremling, K.: Methods of Seawater Analysis, 2nd Edition, Verlag Chemie Weinhein, New York, 419 p., 1983.

Grasshoff, K., Kremling, K., and Ehrhardt, M.: Methods of seawater analysis (3rd edn.), Weinheim Press, WILEY-VCH, 203–273, 1999.

Grégoire, M., Oschlies, A., Canfield, D., Castro, C., Ciglenečki, I., Croot, P., Salin, K., Schneider, B., Serret, P., Slomp, C.P., Tesi, T., Yücel, M. (2023). Ocean Oxygen: the role of the Ocean in the oxygen we breathe and the threat of deoxygenation. Rodriguez Perez, A., Kellett, P., Alexander, B., Muñiz Piniella, Á., Van Elslander, J., Heymans, J. J., [Eds.] Future Science Brief No. 10 of the European Marine Board, Ostend, Belgium. ISSN: 2593-5232. ISBN: 9789464206180. DOI: 10.5281/zenodo.7941157, 2023.

Guy, S.-V., Kress, N., Silverman, J., Gertner, Y., Ozer, T., Biton, E., Lazar, A., Gertman, I., Rahav, E., and Herut, B.: Post-eastern Mediterranean Transient Oxygen Decline in the Deep Waters of the Southeast Mediterranean Sea Supports Weakening of Ventilation Rates, Front. Mar. Sci., 7, https://doi.org/10.3389/FMARS.2020.598686, 2021.

Hainbucher, D., Rubino, A., Cardin, V., Tanhua, T., Schroeder, K., and Bensi, M.: Hydrographic situation during cruise M84/3 and P414 (spring 2011) in the Mediterranean Sea, Ocean Sci., 10, 669-682, https://doi.org/10.5194/os-10-669-2014, 2014.

Helen, R., Powley., Krom, M. D., Van Cappellen, P.: Circulation and oxygen cycling in the Mediterranean Sea: Sensitivity to future climate change, J. Geophys. Res., https://doi.org/10.1002/2016JC012224, 2016.

Hoppema, M., Velo, A., van Heuven, S., Tanhua, T., Key, R. M., Lin, X., Bakker, D. C. E., Perez, F. F., Ríos, A. F., Lo Monaco, C., Sabine, C. L., Álvarez, M., and Bellerby, R. G. J.: Consistency of cruise data of the CARINA database in the Atlantic sector of the Southern Ocean, Earth Syst. Sci. Data, 1, 63–75, https://doi.org/10.5194/essd-1-63-2009, 2009.

Janzen, C., Murphy, D., and Larson, N.: Getting more mileage out of dissolved oxygen sensors in long-term moored applications, OCEANS 2007, IEEE, doi: 10.1109/OCEANS.2007.4449398, 2007.

Johnson, G. C., Robbins, P. E., and Hufford, G. E.: Systematic adjustments of hydrographic sections for internal consistency, J. Atmos. Ocean. Tech., 18, 1234–1244, https://doi.org/10.1175/1520-0426(2001)018<1234:SAOHSF>2.0.CO;2, 2001.

Jullion, L.: TAlPro2016: A Tyrrhenian Sea & Alger-Provençal component of the MedSHIP Programme, RV Angeles Alariño, 18/08/16 – 29/08/16, Palermo (Italy) – Barcelona (Spain), Bremerhaven, EUROFLEETS2 Cruise Summary Report, https://epic.awi.de/id/eprint/49725/, 2016.

Keeling, R. F., Körtzinger, A., and Gruber, N.: Ocean deoxygenation in a warming world, Annu. Rev. Mar. Sci., 2, 199-229, doi: 10.1146/annurev.marine.010908.163855, 2010.

Key, R.M., Tanhua, T., Olsen, A., Hoppema, M., Jutterström, S., Schirnick, C., Van Heuven, S., Kozyr, A., Lin, X., Velo, A., Wallace, D.W.R., Mintrop, L., 2010. The CARINA data synthesis project: introduction and overview. Earth Syst. Sci. Data, 2, 105–121, https://doi.org/10.5194/essd-2-105-2010, 2010.

693 Key, R. M., Kozyr, A., Sabine, C. L., Lee, K., Wanninkhof, R., Bullister, J. L., Feely, R. A., Millero, F. J., Mordy,
694 C., and Peng, T.-H.: A global ocean carbon climatology: Results from Global Data Analysis Project (GLODAP),
695 *Global Biogeochem. Cycles*, 18, GB4031, https://doi.org/10.1029/2004GB002247, 2004.

696 Langdon, C.: Determination of Dissolved Oxygen in Seawater by Winkler Titration using Amperometric
697 Technique, In: Hood, E.M., Sabine, C.L., Sloyan, B.M. (Eds.), The GO-SHIP Repeat Hydrography Manual: A
698 Collection of Expert Reports and Guidelines, Version 1, IOCCP Report Number 14, ICPO Publication Series
699 Number 134, 18pp., https://doi.org/10.25607/OBP-1350, 2010.

700 Lauvset, S. K., and Tanhua, T.: A toolbox for secondary quality control on ocean chemistry and hydrographic data,
701 Limnol. Oceanogr. Methods, 13, 601–608, https://doi.org/10.1002/lom3.10050, 2015.

702 Lauvset, S. K., Lange, N., Tanhua, T., Bittig, H. C., Olsen, A., Kozyr, A., Álvarez, M., Azetsu-Scott, K., Brown,
703 P. J., Carter, B. R., Cotrim da Cunha, L., Hoppema, M., Humphreys, M. P., Ishii, M., Jeansson, E., Murata, A.,
704 Müller, J. D., Pérez, F. F., Schirnick, C., Steinfeldt, R., Suzuki, T., Ulfsbo, A., Velo, A., Woosley, R. J., and Key,
705 R. M.: The annual update GLODAPv2.2023: the global interior ocean biogeochemical data product, Earth Syst.
706 Sci. Data, 16, 2047–2072, https://doi.org/10.5194/essd-16-2047-2024, 2024.

707 Li P and Tanhua T (2020) Recent Changes in Deep Ventilation of the Mediterranean Sea; Evidence From Long-
708 Term Transient Tracer Observations. Front. Mar. Sci. 7:594. doi: 10.3389/fmars.2020.00594

709 Liu G., Yu,X., Zhang,J., Wang,X., Xu,N., Ali,S.: Reconstruction of the three-dimensional dissolved oxygen and
710 its spatio-temporal variations in the Mediterranean Sea using machine learning, Journal of Environmental
711 Sciences,2025,ISSN 1001-0742,https://doi.org/10.1016/j.jes.2025.01.010.

712 López-Jurado, J. L., Balbín, R., Alemany, F., Amengual, B., Aparicio-González, A., Fernández de Puelles, M. L.,
713 García-Martínez, M. C., Gazá, M., Jansá, J., Morillas-Kieffer, A., Moyá, F., Santiago, R., Serra, M., and Vargas-
714 Yáñez, M.: The RADMED monitoring programme as a tool for MSFD implementation: towards an ecosystem-
715 based approach, Ocean Sci., 11, 897–908, https://doi.org/10.5194/os-11-897-2015, 2015.

716 Manca, B., Burca, M., Giorgetti, A., Coatanoan, C., Garcia, M. J., and Iona, A. Physical and biochemical averaged
717 vertical profiles in the Mediterranean regions: an important tool to trace the climatology of water masses and to
718 validate incoming data from operational oceanography, J. Mar. Syst., 48, 83–116,
719 https://doi.org/10.1016/j.jmarsys.2003.11.025, 2004.

720 Macias, D., Garcia-Gorriz, E., and Stips, A.: Deep winter convection and phytoplankton dynamics in the NW
721 Mediterranean Sea under present climate and future (horizon 2030) scenarios, Sci. Rep., 8, 6626,
722 https://doi.org/10.1038/s41598-018-24978-5, 2018.

723 Margirier, F., Testor, P., Heslop, E., Mallil, K., Bosse, A., Houpert, L., Mortier, L., Bouin, M.-N., Coppola, L.,
724 D'Ortenzio, F., Durrieu de Madron, X., Mourre, B., Prieur, L., Raimbault, P., and Taillandier, V.: Abrupt warming
725 and salinification of intermediate waters interplays with decline of deep convection in the Northwestern
726 Mediterranean Sea, *Sci. Rep.*, 10, 20923, https://doi.org/10.1038/s41598-020-77961-9, 2020.

727 Martínez, J., Leonelli, F. E., García-Ladona, E., Garrabou, J., Kersting, D. K., Bensoussan, N., and Pisano, A.:
728 Evolution of marine heatwaves in warming seas: the Mediterranean Sea case study, Front. Mar. Sci., 10, 1193164,
729 https://doi.org/10.3389/fmars.2023.1193164, 2023.

730 Marullo, S., De Toma, V., di Sarra, A., Iacono, R., Landolfi, A., Leonelli, F., Napolitano, E., Meloni, D., Organelli,
731 E., Pisano, A., Santoleri, R., and Sferlazzo, D.: Has the frequency of Mediterranean Marine Heatwaves really
732 increased in the last decades? , EGU General Assembly 2023, Vienna, Austria, 23–28 Apr 2023, EGU23-4429,
733 https://doi.org/10.5194/egusphere-egu23-4429 , 2023.

734 Mavropoulou, A.-M., Vervatis, V., and Sofianos, S.: Dissolved oxygen variability in the Mediterranean Sea, J.
735 Mar. Syst., 208, 103348, https://doi.org/10.1016/j.jmarsys.2020.103348 ,2020.

736 Mavropoulou, A.-M.: Mediterranean Sea: Dissolved Oxygen, Temperature and Salinity Annual Variability and
737 Monthly Climatology for the period 1960-2011, https://doi.org/10.5281/zenodo.3878076 , 2020.

Middleton, L., Wu, W., Johnston, T. M. S., Tarry, D. R., Farrar, J. T., Poulain, P.-M., Özgökmen, T. M., Shcherbina, A. Y., Pascual, A., McNeill, C. L., Belgacem, M., Berta, M., Abbott, K., Worden, A. Z., Wittmers, F., Kinsella, A., Centurioni, L. R., Hormann, V., Cutolo, E., Tintoré, J., Ruiz, S., Casas, B., Cheslack, H., CALYPSO Collaboration, D'Asaro, E. A., and Mahadevan, A.: Ocean cyclone splitting ventilates the upper ocean, Sci. Adv., accepted, 2025.

Moriarty, J. M., Harris, C. K., Fennel, K., Friedrichs, M. A. M., Xu, K., and Rabouille, C.: The roles of resuspension, diffusion and biogeochemical processes on oxygen dynamics offshore of the Rhône River, France: a numerical modeling study, Biogeosciences, 14, 1919–1946, https://doi.org/10.5194/bg-14-1919-2017, 2017.

Olsen, A., Key, R. M., van Heuven, S., Lauvset, S. K., Velo, A., Lin, X., Schirnick, C., Kozyr, A., Tanhua, T., Hoppema, M., Jutterström, S., Steinfeldt, R., Jeansson, E., Ishii, M., Pérez, F. F., and Suzuki, T.: The Global Ocean Data Analysis Project version 2 (GLODAPv2) – an internally consistent data product for the world ocean, Earth Syst. Sci. Data, 8, 297–323, https://doi.org/10.5194/essd-8-297-2016 , 2016.

Olsen, A., Lange, N., Key, R. M., Tanhua, T., Bittig, H. C., Kozyr, A., Álvarez, M., Azetsu-Scott, K., Becker, S., Brown, P. J., Carter, B. R., Cotrim da Cunha, L., Feely, R. A., van Heuven, S., Hoppema, M., Ishii, M., Jeansson, E., Jutterström, S., Landa, C. S., Lauvset, S. K., Michaelis, P., Murata, A., Pérez, F. F., Pfeil, B., Schirnick, C., Steinfeldt, R., Suzuki, T., Tilbrook, B., Velo, A., Wanninkhof, R., and Woosley, R. J.: An updated version of the global interior ocean biogeochemical data product, GLODAPv2.2020, Earth Syst. Sci. Data, 12, 3653–3678, https://doi.org/10.5194/essd-12-3653-2020 , 2020.

Olsen, A., Key, R. M., van Heuven, S., Lauvset, S. K., Velo, A., Lin, X., Schirnick, C., Kozyr, A., Tanhua, T., Hoppema, M., Jutterström, S., Steinfeldt, R., Jeansson, E., Ishii, M., Pérez, F. F., and Suzuki, T.: The Global Ocean Data Analysis Project version 2 (GLODAPv2) – an internally consistent data product for the world ocean, Earth Syst. Sci. Data, 8, 297–323, https://doi.org/10.5194/essd-8-297-2016, 2016.

Olsen, A., Lange, N., Key, R. M., Tanhua, T., Álvarez, M., Becker, S., Bittig, H. C., Carter, B. R., Cotrim da Cunha, L., Feely, R. A., van Heuven, S., Hoppema, M., Ishii, M., Jeansson, E., Jones, S. D., Jutterström, S., Karlsen, M. K., Kozyr, A., Lauvset, S. K., Lo Monaco, C., Murata, A., Pérez, F. F., Pfeil, B., Schirnick, C., Steinfeldt, R., Suzuki, T., Telszewski, M., Tilbrook, B., Velo, A., and Wanninkhof, R.: GLODAPv2.2019 – an update of GLODAPv2, Earth Syst. Sci. Data, 11, 1437–1461, https://doi.org/10.5194/essd-11-1437-2019, 2019.

Owens, W. B., and R. C. Millard Jr., 1985: A new algorithm for CTD oxygen calibration. J. Physical Oceanography., 15, 621-631.

Pastor, F., and Khodayar, S.: Marine heat waves: Characterizing a major climate impact in the Mediterranean, EGU General Assembly 2023, Vienna, Austria, 24–28 Apr 2023, EGU23-13058, https://doi.org/10.5194/egusphere-egu23-13058, 2023.

Reale, M., Cossarini, G., Lazzari, P., Lovato, T., Bolzon, G., Masina, S., Solidoro, C., and Salon, S.: Acidification, deoxygenation, and nutrient and biomass declines in a warming Mediterranean Sea, Biogeosciences, 19, 4035-4065, https://doi.org/10.5194/bg-19-4035-2022, 2022.

Ribotti, A., Sorgente, R., Pessini, F., Cucco, A., Quattrocchi, G., and Borghini, M.: Twenty-one years of hydrological data acquisition in the Mediterranean Sea: quality, availability, and research, Earth Syst. Sci. Data, 14, 4187–4199, https://doi.org/10.5194/essd-14-4187-2022 , 2022.

Schroeder, K., Gasparini, G. P., Tangherlini, M., & Astraldi, M.: Deep and intermediate water in the western Mediterranean under the influence of the Eastern Mediterranean Transient. Geophysical Research Letters, 33(21), https://doi.org/10.1029/2006GL027121, 2006.

Schroeder, K., Tanhua, T., Bryden, H., Alvarez, M., Chiggiato, J., and Aracri, S.: Mediterranean Sea Ship-based Hydrographic Investigations Program (Med-SHIP), Oceanography, 28, 12–15, https://doi.org/10.5670/oceanog.2015.71 , 2015.

Schroeder, K., Chiggiato, J., Bryden, H. L., Borghini, M., and Ben Ismail, S.: Abrupt climate shift in the Western Mediterranean Sea. Scientific reports, 6(1), 23009, https://doi.org/10.1038/srep23009, 2016.

784 Loïc Jullion, L., Coppola,L., Bensi, M.,Ursella, L., Santinelli,C., Giani, M., Chiggiato,J., Aly-Eldeen,M.,
785 Assimakopoulou,G., Bachi, G., Bogner, B., Borghini, M., Cardin, V., Cornec, M., Giannakourou, A.,
786 Giannoudi, L., Gogou, A., Golbol, M., Hazan, O., Karthäuser, C., Kralj, M., Krasakopoulou, E., Matić, F.,
787 Mihanović, H., Muslim, S., Papadopoulos, V., Parinos, C., Paulitschke, A., Pavlidou, A., Pitta, E., Protopapa, M. ,
788 Rahav, E., Raveh, O., Renieris, O. , Reyes-Suarez, N.C., Rousselaki, E., Silverman, J., Souvermezoglou, E.,
789 Urbini, L., Christina Zeri,C., and Zervoudaki, S. :Seawater physics and chemistry along the Med-SHIP transects
790 in the Mediterranean Sea in 2016. Scientific data, 11(1), 52, https://doi.org/10.1038/s41597-023-02835-3, 2024.

791 Schneider, A., Tanhua, T., Roether, W., and Steinfeldt, R.: Changes in ventilation of the Mediterranean Sea during
792 the past 25 year, Ocean Sci., 10, 1–16, https://doi.org/10.5194/os-10-1-2014, 2014.

793 Schroeder, K., Kovačević, V., Civitarese, G., Velaoras, D., Álvarez, M., Tanhua, T., Jullio, L., Coppola, L., Bensi,
794 M., Ursella, L., Santinelli, C., Giani, M., Chiggiato, J., Aly-Eldeen, M., Assimakopoulou, G., Bachi, G., Bogner,
795 B., Borghini, M., Cardin, V., Cornec, M., Giannakourou, A., Giannoudi, L., Gogou, A., Golbol, M., Or Hazan, O.,
796 Karthäuser, C., Kralj, M., Krasakopoulou, E., Matić, F., Mihanović, H., Muslim, S., Papadopoulos, V.P., Parinos,
797 C., Paulitschke, A., Pavlidou, A., Pitta, E., Protopapa, M., Rahav, E., Raveh, O., Renieris, P., Reyes-Suarez, N.
798 C., Rousselaki, E., Silverman, J., Souvermezoglou, E., Urbini, L., Zer, C., and Zervoudaki, S.: Seawater physics
799 and chemistry along the Med-SHIP transects in the Mediterranean Sea in 2016, Sci. Data, 11, 52,
800 https://doi.org/10.1038/s41597-023-02835-3, 2024.

801 Schroeder, K.: TAlPro2022 CRUISE REPORT R/V BELGICA Cruise n. 2022/12 (Version 1), Zenodo,
802 https://doi.org/10.5281/zenodo.6918731 , 2022.

803 Tanhua, T., Brown, P. J., and Key, R. M.: CARINA: nutrient data in the Atlantic Ocean, Earth Syst. Sci. Data, 1,
804 7–24, https://doi.org/10.5194/essd-1-7-2009 , 2009.

805 Tanhua, T.: Matlab Toolbox to Perform Secondary Quality Control (2nd QC) on Hydrographic Data, ORNL
806 CDIAC-158, Carbon Dioxide Inf. Anal. Center, Oak Ridge Natl. Lab., U.S. Dep. Energy, Oak Ridge, Tennessee,
807 158, https://doi.org/10.1002/lom3.10050 , 2010.

808 Tanhua, T.: Hydrochemistry of water samples during MedSHIP cruise Talpro, PANGAEA,
809 https://doi.org/10.1594/PANGAEA.902293 , 2019a.

810 Tanhua, T.: Physical oceanography during MedSHIP cruise Talpro [dataset], PANGAEA,
811 https://doi.org/10.1594/PANGAEA.902330 , 2019b.

812 Testor, P., Bosse, A., Houpert, L., Margirier, F., Mortier, L., Legoff, H., Dausse, D., Labaste, M., Bouin, M.-N.,
813 Coppola, L., Koenig, Z., Damien, P., et al.: Multiscale observations of deep convection in the northwestern
814 Mediterranean Sea during winter 2012–2013 using multiple platforms, *J. Geophys. Res.-Oceans*, 122, 1745–1776,
815 https://doi.org/10.1002/2016JC012671, 2017.

816 Uchida, H. Johnson, G. C. and McTaggart, G. C.: CTD Oxygen Sensor Calibration Procedures. In, The GO-SHIP
817 Repeat Hydrography Manual: A Collection of Expert Reports and Guidelines. Version 1, (eds Hood, E.M., C.L.
818 Sabine, and B.M. Sloyan), 17pp. (IOCCP Report Number 14; ICPO Publication Series Number 134),
819 https://doi.org/10.25607/OBP-1344, 2010.

820 Ulses, C., D'Ortenzio, F., Coppola, L., Estournel, C., Testor, P., Marsaleix, P., Prieur, L., Taillandier, V., Dumas,
821 F., Severin, T., and Conan, P.: Oxygen budget of the north-western Mediterranean deep-convection region,
822 *Biogeosciences*, 18, 937–960, https://doi.org/10.5194/bg-18-937-2021, 2021.

823 Yao, M., Marcou, O., Goyet, C., Guglielmi, V., Touratier, F., and Savy, J.-P.: Time variability of the north-western
824 Mediterranean Sea pH over 1995–2011, Mar. Environ. Res., 116, 51–60,
825 https://doi.org/10.1016/j.marenvres.2016.02.016, 2016.